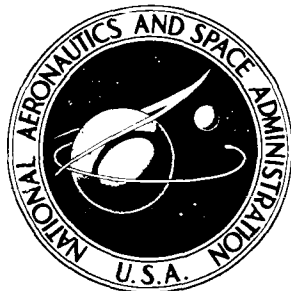


NASA TECHNICAL
MEMORANDUM

NASA TM X-2623



NASA TM X-2623

FILE COPY

LOW-SPEED AERODYNAMIC CHARACTERISTICS
OF NACA 6716 AND NACA 4416 AIRFOILS WITH
35-PERCENT-CHORD SINGLE-SLOTTED FLAPS

by Gene J. Bingham and Kevin W. Noonan

Langley Directorate

U.S. Army Air Mobility R&D Laboratory

Hampton, Va. 23665



NATIONAL AERONAUTICS AND SPACE ADMINISTRATION • WASHINGTON, D. C. • MAY 1974

1. Report No. NASA TM X-2623	2. Government Accession No.	3. Recipient's Catalog No.	
4. Title and Subtitle LOW-SPEED AERODYNAMIC CHARACTERISTICS OF NACA 6716 AND NACA 4416 AIRFOILS WITH 35-PERCENT-CHORD SINGLE-SLOTTED FLAPS		5. Report Date May 1974	
7. Author(s) Gene J. Bingham and Kevin W. Noonan, Langley Directorate, U.S. Army Air Mobility R&D Laboratory		6. Performing Organization Code	
9. Performing Organization Name and Address NASA Langley Research Center Hampton, Va. 23665		8. Performing Organization Report No. L-8410	
		10. Work Unit No. 760-17-01-10	
		11. Contract or Grant No.	
		13. Type of Report and Period Covered Technical Memorandum	
12. Sponsoring Agency Name and Address National Aeronautics and Space Administration Washington, D.C. 20546		14. Sponsoring Agency Code	
15. Supplementary Notes The information presented herein was previously made available to the U.S. military air services.			
16. Abstract An investigation has been conducted in the Langley low-turbulence pressure tunnel to determine the two-dimensional lift and pitching-moment characteristics of an NACA 6716 and an NACA 4416 airfoil with 35-percent-chord single-slotted flaps. Both models were tested with flaps deflected from 0° to 45°, at angles of attack from -6° to several degrees past stall, at Reynolds numbers from 3.0×10^6 to 13.8×10^6 , and primarily at a Mach number of 0.23. Tests were also made to determine the effect of several slot entry shapes on performance.			
17. Key Words (Suggested by Author(s)) NACA airfoils High Reynolds number Low-speed aerodynamics		18. Distribution Statement Unclassified – Unlimited	
STAR Category 01			
19. Security Classif. (of this report) Unclassified	20. Security Classif. (of this page) Unclassified	21. No. of Pages 50	22. Price* \$3.25

LOW-SPEED AERODYNAMIC CHARACTERISTICS
OF NACA 6716 AND NACA 4416 AIRFOILS WITH 35-PERCENT-CHORD
SINGLE-SLOTTED FLAPS*

By Gene J. Bingham and Kevin W. Noonan
Langley Directorate, U.S. Army Air Mobility R&D Laboratory

SUMMARY

An investigation has been conducted in the Langley low-turbulence pressure tunnel to determine the two-dimensional lift and pitching-moment characteristics of an NACA 6716 and an NACA 4416 airfoil with 35-percent-chord single-slotted flaps. Both models were tested with flaps deflected from 0° to 45° , at angles of attack from -6° to several degrees past stall, at Reynolds numbers from 3.0×10^6 to 13.8×10^6 , and primarily at a Mach number of 0.23. Tests were also made to determine the effect of several slot entry shapes on performance.

The results of this investigation indicate that with the flap retracted, the maximum lift coefficient for the NACA 6716 airfoil was about 2.1 and that for the NACA 4416 airfoil was about 1.8. With the flap deflected 40° and slot entry 1, the maximum lift coefficients were 3.9 and 4.1 for the NACA 6716 and NACA 4416 airfoils, respectively. For the other two slot entry shapes investigated, the maximum lift coefficient with deflected flaps decreased by about 0.1. An increase of about 0.2 in maximum lift coefficient was obtained for the NACA 4416 airfoil by increasing the flap slot width from the design value and hence changing the slot performance.

The pitching-moment coefficients for the NACA 6716 airfoil were more negative at all flap angles by about -0.1 than those for the NACA 4416 airfoil. Deflection of the flap on the NACA 6716 airfoil from 0° to 40° decreased the pitching-moment coefficient from about -0.2 to -0.8.

*The information presented herein was previously made available to the U.S. military air services.

INTRODUCTION

The NASA has recently resumed subsonic and transonic two-dimensional airfoil research. The Langley low-turbulence pressure tunnel, which was originally constructed to test two-dimensional airfoils (ref. 1), was reactivated recently to continue testing airfoils at low speeds and high Reynolds numbers. Because of the Reynolds number capability of this tunnel, NASA conducted a two-dimensional wind-tunnel test of two airfoil configurations. The primary objective of this investigation was to determine the lift characteristics of the NACA 6716 and 4416 airfoils with 35-percent-chord single-slotted flaps.

The two airfoils were tested in the Langley low-turbulence pressure tunnel primarily at a Mach number of 0.23 and Reynolds numbers (based on airfoil chord) between 3.0×10^6 and 13.8×10^6 . The investigation included three different slot entry shapes, several different slot widths, and flap deflections from fully retracted to 45° . The NACA 4416 airfoil with flap retracted was investigated with a boundary-layer transition strip at 5 percent chord. Lift and pitching-moment coefficients were determined from measurements of the static pressures on the airfoil surface.

SYMBOLS

The units used for the physical quantities of this paper are given both in the International System of Units (SI) and in the U.S. Customary Units. The measurements and calculations were made in the U.S. Customary Units.

C_p static-pressure coefficient, $\frac{p_l - p_\infty}{q_\infty}$

c airfoil chord, 0.6096 m (24.00 in.)

c_c section chord-force coefficient (obtained by C_p integrations)

c_l section lift coefficient, $c_n \cos \alpha - c_c \sin \alpha$

c_m section pitching-moment coefficient about quarter-chord
(obtained by C_p integrations)

$c_{m,f}$	section pitching-moment coefficient about leading edge of flap (obtained by C_p integrations)
c_n	section normal-force coefficient (obtained by C_p integrations)
$\frac{dC_l}{d\alpha_0}$	lift-curve slope at $\alpha = 0^\circ$
M	Mach number
p	static pressure, N/m ² (lbf/ft ²)
q	dynamic pressure, $\frac{1}{2}\rho V^2$, N/m ² (lbf/ft ²)
R	Reynolds number based on airfoil chord
V	velocity, m/sec (ft/sec)
x,y	airfoil coordinates, cm (in.)
α	angle of attack, angle between chord line from leading edge to trailing edge and airstream axis, deg
δ_f	flap deflection angle measured relative to flap chord at zero deflection, deg
ρ	density, kg/m ³ (slugs/ft ³)

Subscripts:

f	flap
l	local
le	leading edge
max	maximum
∞	free stream

Abbreviations:

L.E. leading edge

SE slot entry

APPARATUS AND PROCEDURE

Model Description

The two airfoil configurations investigated (fig. 1) were NACA four-digit-series airfoils (NACA 6716 and 4416) equipped with $0.35c$ single-slotted flaps. The airfoil coordinates, which were derived by the method described in references 2 and 3, are presented in table I.

The flap coordinates behind about $0.88c$ on the upper surface and about $0.74c$ on the lower surface were the same as those of the basic wing for both models. (See fig. 2.) The forward parts of the flaps were made of other NACA four-digit-series airfoil sections (table II): The NACA 8718 airfoil section was used with the NACA 6716 airfoil, and the NACA 4418 airfoil section was used with the NACA 4416 airfoil. At the juncture, the contour of the front section of the flap was faired into the aft contour of the flap. The resultant incidence of the flap chord was 6.45° for the NACA 6716 airfoil section and 1.00° for the NACA 4416 airfoil section. (See fig. 1.)

The airfoils were tested at flap deflection angles of 0° , 25° , 30° , 35° , 40° , and 45° measured relative to the chord line of the retracted flap. The NACA 6716 airfoil was also tested at a flap deflection angle of 50.5° . At this flap deflection, the flap leading edge extended above the upper surface of the airfoil to provide high drag and to spoil the lift and thereby to minimize landing ground-roll distance.

All flap positions and deflection angles were fixed by brackets, which transmitted the flap loads to the main wing section. (See figs. 3 and 4.) The flap leading-edge positions tested for both airfoils are presented in table III.

The three slot entry shapes were designated SE 1, SE 2, and SE 3. (See fig. 2.) The basic shape (SE 1) was a smooth entrance with a gap between the entry (or lower surface of the wing) and the lower surface of the retracted flap.

The alternate entry shapes (SE 2 and SE 3) provided a smooth, uninterrupted surface at the wing-flap lower surface juncture and had identical geometry when the flap was retracted. Their differences occurred when the flap was deflected. The SE 2 entry shape was designed as a hinged panel that translated aft from the flap retracted position and rotated to provide a smooth entry when the flap was extended. (See fig. 2.) The SE 3 had

fixed geometry and therefore precluded a smooth slot entry during all flap deflection modes of operation.

The airfoil models (fig. 3) were machined from solid aluminum billets, and each had a chord of 0.6096 meter (24.00 in.) and a span of 1.002 meters (39.44 in.). Each had 78 surface orifices located as shown in table IV. Sixty-six orifices were located at 1/2 span (center line), six were at 1/3 span, and six were at 2/3 span. The orifices were drilled perpendicular to the local surface and had diameters of 0.8128 mm (0.032 in.).

Wind Tunnel

The Langley low-turbulence pressure tunnel (ref. 1) is a closed-throat, single-return tunnel, which can be operated at stagnation pressures from 1 to 10 atm (1 atm = 101.325 kN/m^2). At 1 atm the attainable Mach number and Reynolds number are 0.46 and 6.6×10^6 per meter (2×10^6 per foot), respectively; at 10 atm the corresponding values are 0.23 and 49×10^6 per meter (15×10^6 per foot). The test section is 0.914 meter (3 ft) wide by 2.286 meters (7.5 ft) high.

The models are attached to circular sidewall plates, which are rotated to obtain the desired angle of attack (fig. 3); wall boundary-layer control is not employed. The sidewall plates are 1.015 meters (3.33 ft) in diameter and are flush with the tunnel wall. Airfoil models are mounted to span the tunnel width with their quarter-chord coincident with the axis of the circular plate.

Instrumentation

Measurements of the static pressures on the airfoil surface were made by an automated pressure-scanning system and recorded on punched cards. Basic tunnel pressures (stagnation pressure and stagnation pressure minus reference static pressure) were measured with precision transducers and recorded on punched cards. Angle of attack was determined from the output of a calibrated potentiometer attached to the circular sidewall plates which support each model.

Test Procedures

All configurations were tested with polished surfaces; however, one configuration, the NACA 4416 airfoil with flap retracted and the juncture sealed and faired, was tested with a transition strip on both upper and lower surfaces. The transition strip, which was selected on the basis of reference 4, extended 3.17 mm (0.125 in.) rearward from the 0.05c station and consisted of sparsely spaced carborundum grit (0.711 mm (0.028 in.) diameter) attached to the airfoil surface with lacquer.

The measurements of the static pressures on the wing and flap surfaces were reduced to standard pressure coefficients and then machine integrated to obtain section

normal-force coefficient, section chord-force coefficient, and pitching-moment coefficient about both the leading edge and the quarter-chord.

Airfoil wake pressures were obtained with a wake survey rake for some test conditions, but the unsteadiness of the wake caused by trailing-edge flow separation even at low angles of attack ($<40^\circ$) precluded an accurate determination of the drag by this method. For this reason, drag is not presented in this report.

The wind-tunnel boundary corrections calculated by the method of reference 5 are

$$c_l \text{ (corrected)} = 0.976 c_l$$

$$c_m \text{ (corrected)} = 0.991 c_m + 0.004 c_l$$

$$\alpha \text{ (corrected)} = \alpha + 0.133(c_l + 4c_m)$$

The corrections are estimated to be within the accuracy of the data and therefore have not been applied.

RESULTS

The results of this investigation have been reduced to coefficient form and are presented as follows:

Airfoil	Slot entry	Flap deflection, deg	Mach number	Reynolds number	Control variable	Figure
Plots of C_p against x/c						
6716	SE 1	0	0.23	12×10^6	α	5(a)
6716		30				5(b)
4416		0				5(c)
4416		30				5(d)
Plot of c_l and c_m against α						
6716	SE 1	0	0.23	Varied	R	6(a)
		30				6(b)
		40				6(c)
	Varied			Varied	δ_f	6(d)
	SE 3	0		Varied	R	6(e)
	SE 3 sealed			Varied	R	6(f)
	SE 3			12×10^6	Slot seal	6(g)
	SE 3	30		Varied	R	6(h)
	SE 2	30		Varied	R	6(i)
	Varied	0		12×10^6	Slot entry	6(j)
	Varied	30		12×10^6	Slot entry	6(k)
	SE 3 sealed	0		7×10^6	M	6(l)
4416	SE 1	0	0.23	Varied	R	7(a)
		30				7(b)
		40				7(c)
	Varied			12.8×10^6	δ_f	7(d)

Airfoil	Slot entry	Flap deflection, deg	Mach number	Reynolds number	Control variable	Figure
Plot of c_l and c_m against α						
4416	SE 3	0	0.23	Varied	R	7(e)
	SE 3 sealed	↓		Varied	R	7(f)
	SE 3	↓		12×10^6	Slot seal	7(g)
	SE 3	30		Varied	R	7(h)
	SE 2	30		Varied	R	7(i)
	Varied	0		12×10^6	Slot entry	7(j)
	Varied	30		12×10^6	Slot entry	7(k)
	SE 3 sealed	0		7×10^6	Transition	7(l)
	SE 3 sealed	0		9×10^6	Transition	7(m)
	SE 1	30		12×10^6	Flap leading-edge position	7(n)
		↓			↓	7(o)
		0				7(p)
		30				7(q)
		40			Airfoil	8(a)
	SE 3	0				8(b)
	SE 3 sealed	0				8(c)
	SE 3	30				8(d)
	SE 2	30				8(e)
		↓				8(f)
		0				8(g)
Plot of $dc_l/d\alpha_0$ against δ_f						
Varied	SE 1	Varied	0.23	12×10^6	Airfoil	9
Plot of $(c_l)_{max}$ against R						
6716	Varied	Varied	0.23	Varied	SE, δ_f	10(a)
4416	Varied	Varied	.23	Varied	SE, δ_f	10(b)
Plot of $(c_l)_{max}$ against $(x/c)_{le}$						
4416	SE 1	30	0.23	12×10^6	$(y/c)_{le}$	11
Plot of c_m against δ_f						
Varied	SE 1	Varied	0.23	12×10^6	Airfoil	12
Plot of $c_{m,f}$, $c_{n,f}$, and $c_{c,f}$ against α						
6716	SE 1	Varied	0.23	12×10^6	δ_f	13(a)
4416	SE 1	Varied	.23	12×10^6	δ_f	13(b)

DISCUSSION

Pressure Distributions

Representative static-pressure distributions for the NACA 6716 and 4416 airfoil sections with $0.35c$ single-slotted flaps are presented in figure 5 for flap deflections of 0° and 30° . A noteworthy feature of the pressure distributions is observed at $\delta_f = 0^\circ$: The upper surface pressures for both airfoils are nearly uniform behind $x/c = 0.95$ for angles of attack of 0° and 4° . This lack of pressure gradient is an indication of local boundary-layer separation. All pressure data have been examined, and they indicate similar characteristics for each slot entry shape (including sealed and faired) at all Reynolds numbers.

Lift Characteristics

The slope of the lift curves (figs. 6, 7, and 8) at $\alpha = 0^\circ$ for the NACA 6716 and 4416 airfoils with slot entry 1 are presented in figure 9. At $\delta_f = 0^\circ$ the slope for the NACA 6716 airfoil is 0.094 per degree, compared with 0.107 per degree for the NACA 4416 airfoil; the same values were observed with the other slot entries (figs. 6(j) and 7(j)). The slope is greater for the NACA 4416 airfoil for all corresponding flap deflections and slot entry configurations (for example, figs. 6(k) and 7(k)).

The variations of maximum lift coefficient $(c_l)_{\max}$ with test Reynolds number are summarized in figure 10; $(c_l)_{\max}$ generally increases with Reynolds number because of the well-known decrease in viscous effects. For the NACA 6716 airfoil with flap retracted (fig. 10(a)), $(c_l)_{\max}$ is between 2.0 and 2.2 at Reynolds numbers between 7×10^6 and 12×10^6 ; for the NACA 4416 airfoil (fig. 10(b)), the corresponding value is between 1.6 and 1.8. The $(c_l)_{\max}$ is higher for the NACA 6716 airfoil probably because of its greater and more rearward camber. (See ref. 6.) As shown in figures 7(l) and (m), $(c_l)_{\max}$ is reduced to about 1.3 when the transition strip was added at $0.05c$.

With the flap deflected 25° or 30° and slot entry 1, the $(c_l)_{\max}$ for both airfoils is about 3.8. At $\delta_f = 40^\circ$, $(c_l)_{\max}$ values are about 3.9 for the NACA 6716 airfoil and 4.1 for the NACA 4416 airfoil. At $\delta_f = 45^\circ$, $(c_l)_{\max}$ decreases slightly for both airfoils, and a review of the data indicates that this decrease results from a loss in lift of both the wing and the flap.

The 50.5° flap configuration was designed to provide high drag and low lift in order to minimize ground-roll distance from touchdown to taxi speed. The flap leading edge was extended above the airfoil surface (fig. 1) to decrease the upper surface velocity and thus spoil lift (fig. 6(d)). The maximum lift coefficient was not determined for this flap deflection because the model caused severe, unsteady tunnel flow at angle of attack above 12° .

With flaps deflected, the general decrease in $(c_l)_{\max}$ with increasing Reynolds number can be attributed to increased mass flow through the flap slot as a result of a thinner lower surface boundary layer with increasing Reynolds number. This increase in mass flow is believed to alter the velocity vectors in the confluent flow over the flap upper surface which then results in a loss of flap lift because of premature boundary-layer separation. A review of all the static-pressure distributions confirms that the separation point moves forward as Reynolds number is increased. In several instances (for example, figs. 6(h), 6(i), 7(h), and 7(i)), increases in Reynolds number result in a general reduction in lift for the complete angle-of-attack range.

The $(c_l)_{\max}$ for the NACA 4416 airfoil as influenced by changes in flap leading-edge position is shown in figure 11 at the highest test Reynolds number; the design value is shown at $(x/c)_l e = 0.861$ for reference. The $(c_l)_{\max}$ increases from 3.8 to 4.0 as the flap leading edge is moved aft about 2 to 2.5 percent chord and down about 1.2 percent chord. The increase in area and thus in mass flow through the slot passage results in an increase in both wing and flap circulation lift. The increase in area has an adverse effect in some cases (fig. 11). This is probably due to the influence of slot exit flow direction (as controlled by the slot contour) on the flap upper surface boundary-layer separation.

Although configuration and Reynolds number effects are of primary interest in this investigation, a limited amount of data was obtained with the NACA 6716 airfoil to determine the influence of Mach number on the maximum lift coefficient. The data indicate (fig. 6(l)) that $(c_l)_{\max}$ decreases from about 2.1 to 1.9 when the stream Mach number is increased from 0.23 to 0.36. The loss in $(c_l)_{\max}$ results from local supersonic flow in the leading-edge region and an accompanying terminal shock wave. The shock-wave pressure rise thickens the boundary layer and causes separation at lower angles of attack. On the basis of the pressure distribution at $\delta_f = 0^\circ$ (fig. 5(a)) and reference 7, the critical Mach number for the NACA 6716 airfoil at $(c_l)_{\max}$ is predicted to be about 0.28, and the small decrease shown in figure 6(l) at $M = 0.30$ seems to be in agreement with the estimate; the corresponding value for the NACA 4416 airfoil is estimated from figure 5(c) to be about 0.32.

Pitching Moment

The maximum and minimum values of pitching-moment coefficient at angles of attack up to stall have been determined from figures 6, 7, and 8 for both airfoils at each flap deflection angle and for all available test Reynolds numbers. These values are presented in figure 12 at each flap deflection angle to indicate (by the symbol height) the combined influence of angles of attack up to stall, slot entry shape, and in some incidences, Reynolds number. The smaller bandwidth at $\delta_f = 25^\circ$, 35° , and 45° simply reflects that these data do not include Reynolds number influences. At all flap angles the pitching-moment coefficient for the NACA 6716 airfoil is more negative than that for the NACA 4416

airfoil. At $\delta_f = 0^\circ$ the NACA 6716 airfoil had a much larger c_m than the NACA 4416 airfoil (about -0.19 to -0.07) because of the higher aft camber of the 6716 airfoil. The most negative moment coefficients for both airfoils occur at $\delta_f = 40^\circ$ with mean values of about -0.78 for the NACA 6716 airfoil and about -0.74 for the NACA 4416 airfoil.

The pitching-moment coefficient about the flap leading edge and the flap normal-and chord-force coefficients are presented in figure 13. These data can be used to estimate flap hinge-moment coefficients about any selected point.

SUMMARY OF RESULTS

An investigation has been conducted in the Langley low-turbulence pressure tunnel to determine the two-dimensional lift and pitching-moment characteristics of an NACA 6716 and an NACA 4416 airfoil with 35-percent-chord single-slotted flaps. Both airfoil models were tested at a Mach number of 0.23, angles of attack from -6° to several degrees past stall, and Reynolds numbers from 3.0×10^6 to 13.8×10^6 . The NACA 6716 airfoil section was investigated at Mach numbers from 0.23 to 0.36. The effects of flap deflection angle for several slot entry shapes were investigated also. The results of this investigation are summarized as follows:

1. With the flap retracted, the maximum lift coefficient was about 2.1 for the NACA 6716 airfoil and about 1.8 for the NACA 4416 airfoil.
2. With the flap deflected 40° and slot entry 1, the maximum lift coefficients were 3.9 and 4.1 for the NACA 6716 and NACA 4416 airfoils, respectively. For the other two slot entry shapes investigated, the maximum lift coefficient with deflected flaps decreased about 0.1.
3. An increase of about 0.2 in maximum lift coefficient was obtained for the NACA 4416 airfoil by increasing the flap slot width from the design value and hence changing the slot performance.
4. The maximum lift coefficient of the NACA 6716 airfoil decreased from 2.1 to 1.9 when the stream Mach number was increased from 0.23 to 0.36.
5. The pitching-moment coefficients for the NACA 6716 airfoil were more negative at all flap deflection angles by about 0.1 than those for the NACA 4416 airfoil.

Langley Research Center,
National Aeronautics and Space Administration,
Hampton, Va., September 12, 1972.

REFERENCES

1. Von Doenhoff, Albert E.; and Abbott, Frank T., Jr.: The Langley Two-Dimensional Low-Turbulence Pressure Tunnel. NACA TN 1283, 1947.
2. Jacobs, Eastman N.; Ward, Kenneth E.; and Pinkerton, Robert M.: The Characteristics of 78 Related Airfoil Sections From Tests in the Variable-Density Wind Tunnel. NACA Rep. 460, 1933.
3. Abbott, Ira H.; Von Doenhoff, Albert E.; and Stivers, Louis S., Jr.: Summary of Airfoil Data. NACA Rep. 824, 1945.
4. Braslow, Albert L.; and Knox, Eugene C.: Simplified Method for Determination of Critical Height of Distributed Roughness Particles for Boundary-Layer Transition at Mach Numbers From 0 to 5. NACA TN 4363, 1958.
5. Allen, H. Julian; and Vincenti, Walter G.: Wall Interference in a Two-Dimensional-Flow Wind Tunnel, With Consideration of the Effect of Compressibility. NACA Rep. 782, 1944.
6. Loftin, Laurence K., Jr.; and Bursnall, William J.: The Effects of Variations in Reynolds Number Between 3.0×10^6 and 25.0×10^6 Upon the Aerodynamic Characteristics of a Number of NACA 6-Series Airfoil Sections. NACA Rep. 964, 1950. (Supersedes NACA TN 1773.)
7. Von Kármán, Th.: Compressibility Effects in Aerodynamics. J. Aeronaut. Sci., vol. 8, no. 9, July 1941, pp. 337-356.

TABLE I.- DESIGN COORDINATES FOR AIRFOIL SECTIONS

[Stations and ordinates given in percent airfoil chord; leading-edge radius, 0.0282c]

NACA 6716 ^a				NACA 4416 ^b			
Upper surface		Lower surface		Upper surface		Lower surface	
x	y	x	y	x	y	x	y
0	0	0	0	0	0	0	0
.83	2.7	1.67	-2.28	.77	2.72	1.74	-2.23
1.93	3.86	3.07	-3.01	1.85	3.91	3.15	-2.94
4.23	5.51	5.75	-3.85	4.17	5.60	5.83	-3.73
6.65	6.75	8.35	-4.32	6.59	6.89	8.41	-4.17
9.09	7.77	10.91	-4.58	9.07	7.92	10.93	-4.42
14.04	9.36	15.96	-4.77	14.11	9.51	15.89	-4.63
19.07	10.53	20.93	-4.65	19.24	10.61	20.76	-4.61
24.13	11.39	25.87	-4.35	24.41	11.34	25.59	-4.46
29.22	12.01	30.78	-3.92	29.60	11.74	30.40	-4.24
39.43	12.62	40.57	-2.82	40.00	11.74	40.00	-3.74
49.65	12.56	50.35	-1.54	50.16	10.95	49.84	-3.17
59.85	11.96	60.15	-.21	60.27	9.63	59.73	-2.52
70.00	10.89	70.00	1.12	70.32	7.87	69.68	-1.88
80.47	8.80	79.54	1.87	80.31	5.71	79.69	-1.26
90.51	5.20	89.49	1.47	90.21	3.14	89.79	-.70
95.35	2.85	94.65	.82	95.13	1.71	94.87	-.43
100.07	.16	99.93	-.16	100.02	.17	99.98	-.17

^a Slope of radius through leading edge, 0.17.

^b Slope of radius through leading edge, 0.20.

TABLE II.- DESIGN COORDINATES FOR FORWARD PART OF FLAP

[Stations and ordinates given in percent flap chord; leading-edge radius, 0.0356c]

NACA 8718 ^a				NACA 4418 ^b			
Upper surface		Lower surface		Upper surface		Lower surface	
x	y	x	y	x	y	x	y
0	0	0	0	0	0	0	0
.61	3.05	1.88	-2.49	1.25	3.76	1.25	-2.11
1.64	4.39	3.36	-3.27	2.50	5.00	2.50	-2.99
3.89	6.32	6.11	-4.11	5.00	6.75	5.00	-4.06
6.22	7.79	8.78	-4.55	7.50	8.06	7.50	-4.67
8.63	9.01	11.37	-4.77	10.00	9.11	10.00	-5.06
13.57	10.95			15.00	10.66		
18.60	12.41			20.00	11.72		
23.70	13.51			25.00	12.40		
28.83	14.31			30.00	12.76		
39.15	15.19			40.00	12.70		
49.48	15.27			50.00	11.85		
59.78	14.68			60.00	10.44		

^a Used with NACA 6716; slope of radius through leading edge, 0.21.

^b Used with NACA 4416; slope of radius through leading edge, 0.20.

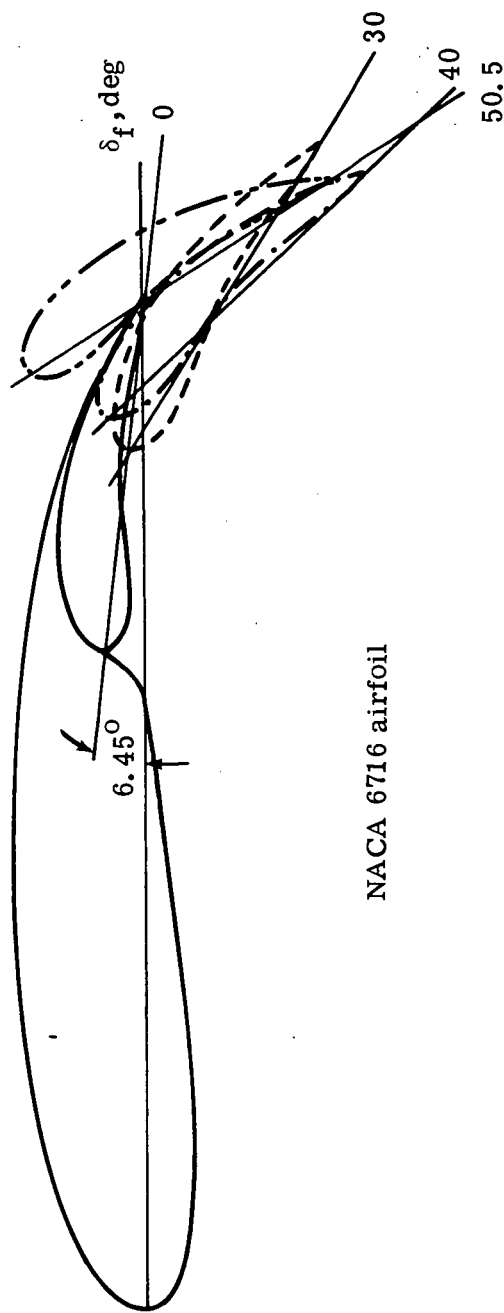
TABLE III.- LOCATION OF FLAP LEADING EDGE

[Stations and ordinates given in percent wing chord]

Airfoil	δ_f , deg	x	y
6716 Basic	0	65.2	3.9
	25	84.9	1.4
	30	86.1	3.3
	35	87.0	3.5
	40	87.7	3.7
	45	88.3	3.7
	50.5	92.2	11.2
4416 Basic	0	65.0	0.7
	25	84.9	1.5
	30	86.2	.7
	35	86.9	.9
	40	87.6	1.1
	45	88.2	1.1
	50.5	92.1	8.6
4416 Matrix	30	87.1	1.5
	30	88.1	1.5
	30	88.6	1.5
	30	87.1	1.0
	30	88.1	1.0
	30	88.6	1.0
	30	87.1	.5
	30	88.1	.5
	30	88.1	.5
	30	87.1	-.5
	30	88.1	-.5
	30	88.6	-.5

TABLE IV.- LOCATIONS OF PRESSURE ORIFICES

Wing		Flap			
Upper surface, percent airfoil chord	Lower surface, percent airfoil chord	Upper surface		Lower surface	
		Percent flap chord	Percent wing chord	Percent flap chord	Percent wing chord
At center line					
0	0.50	0	65.20		
.50	5.00	1.00	65.60	1.00	65.60
5.00	7.50			2.50	66.09
7.50	10.00	5.00	66.96	5.00	66.96
10.00	15.00	7.50	67.83	7.50	67.83
15.00	20.00	13.74	70.00	13.74	70.00
20.00	25.00	20.00	72.18	20.00	72.18
25.00	30.00	28.12	75.00	28.12	75.00
30.00	35.00	35.00	77.40	35.00	77.40
35.00	40.00	42.49	80.00	42.49	80.00
40.00	50.00	50.00	82.61	50.00	82.61
50.00	60.00	62.62	87.00	62.62	87.00
60.00	62.50	71.25	90.00	71.25	90.00
70.00	64.00	80.00	93.05	80.00	93.05
75.00	65.00	90.00	96.52	90.00	96.52
80.00	67.00	100.00	100.00		
87.00	70.00				
	75.00				
	80.00				
	87.00				
At 1/3 span					
25.00	25.00	50.00	82.61	50.00	82.61
50.00	50.00				
At 2/3 span					
25.00	25.00	50.00	82.61	50.00	82.61
50.00	50.00				



NACA 6716 airfoil

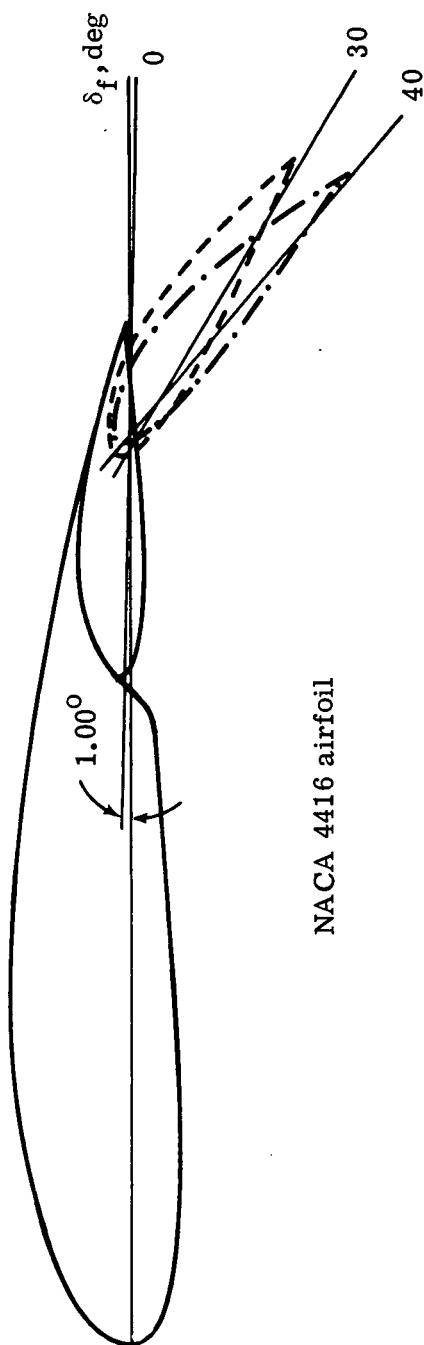
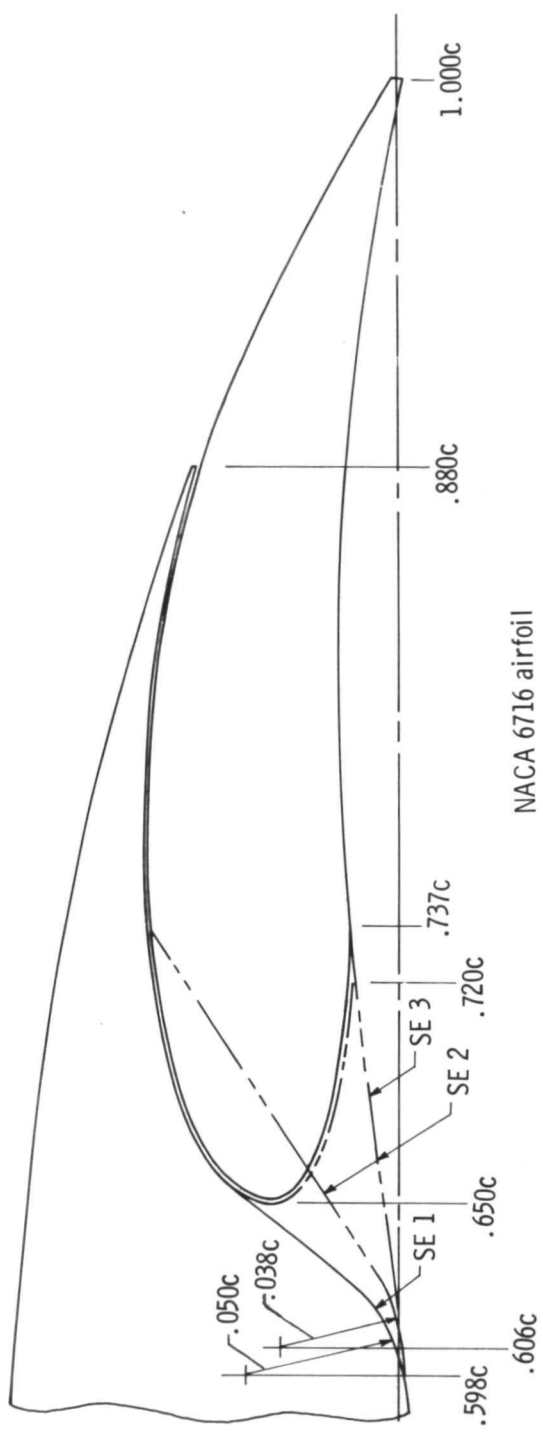
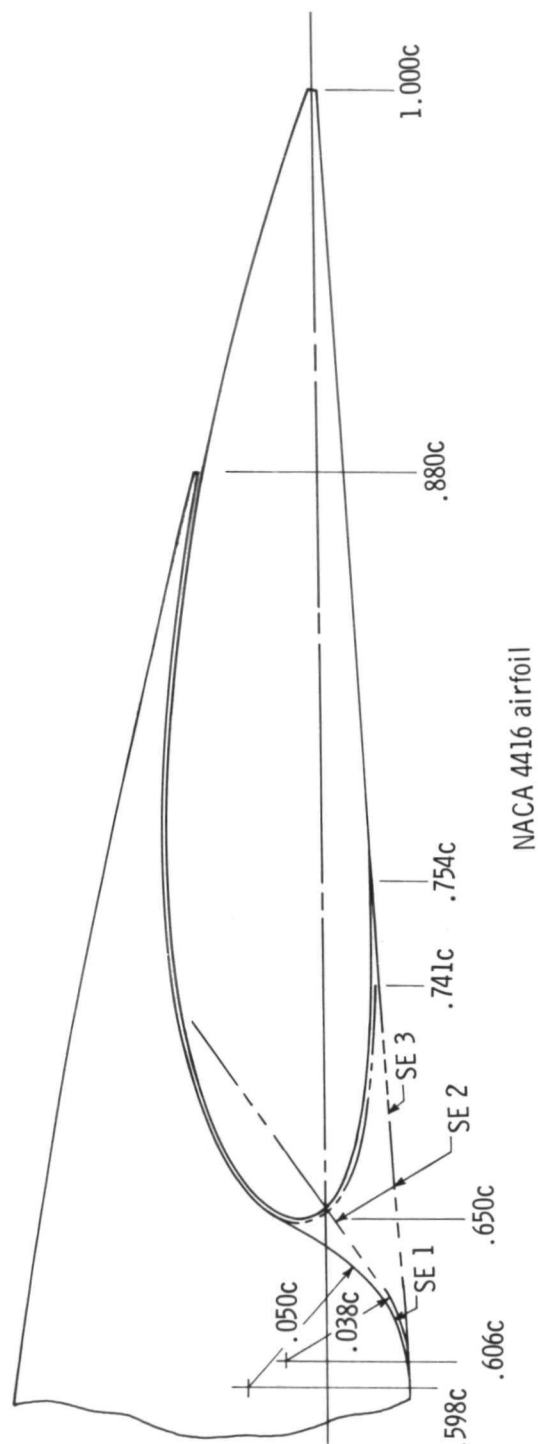


Figure 1.- Airfoil configurations.



NACA 6716 airfoil



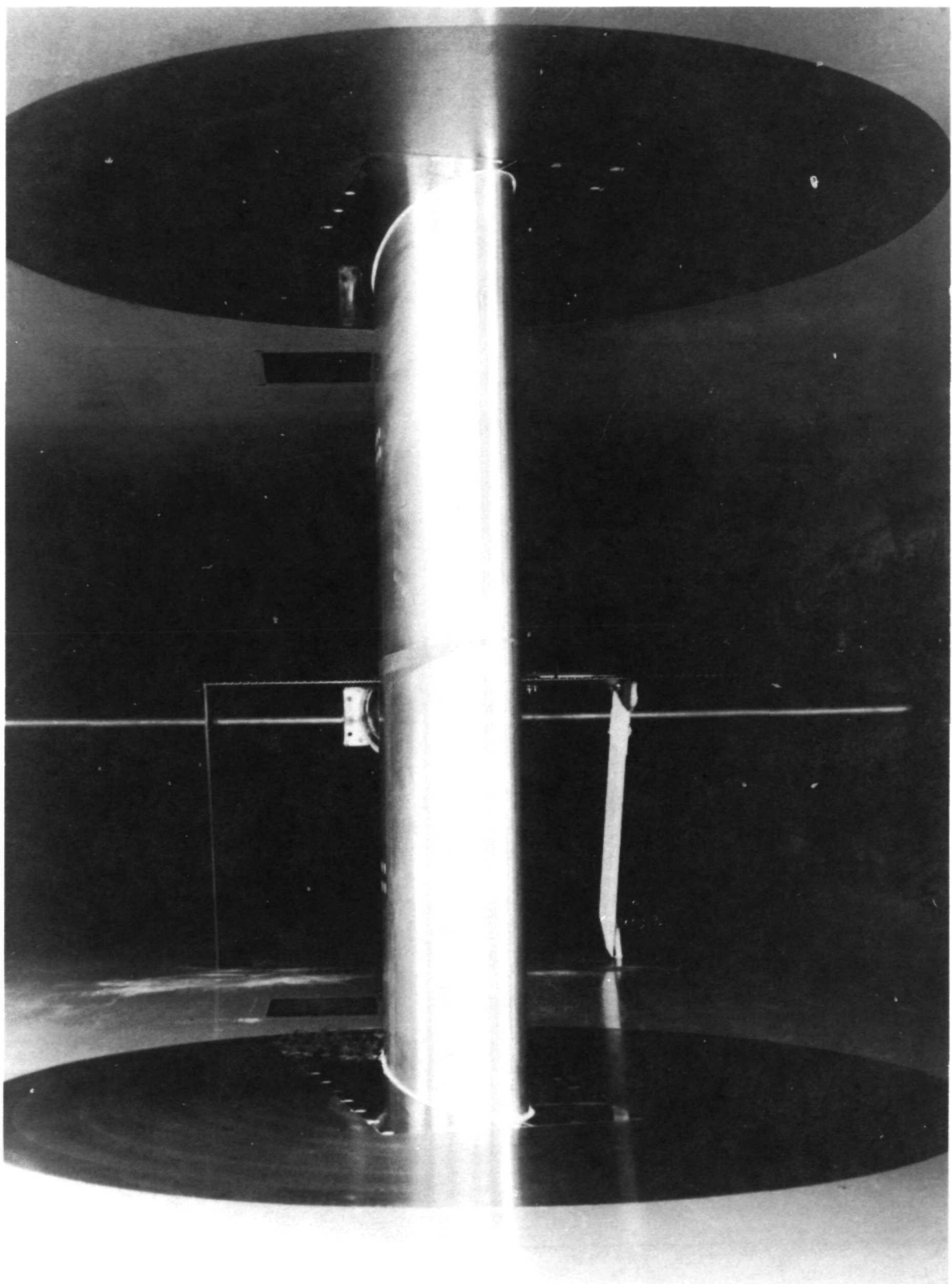
NACA 4416 airfoil

Figure 2.- Flap slot entry shapes.

L-71-2564

(a) Front view of upper surface.

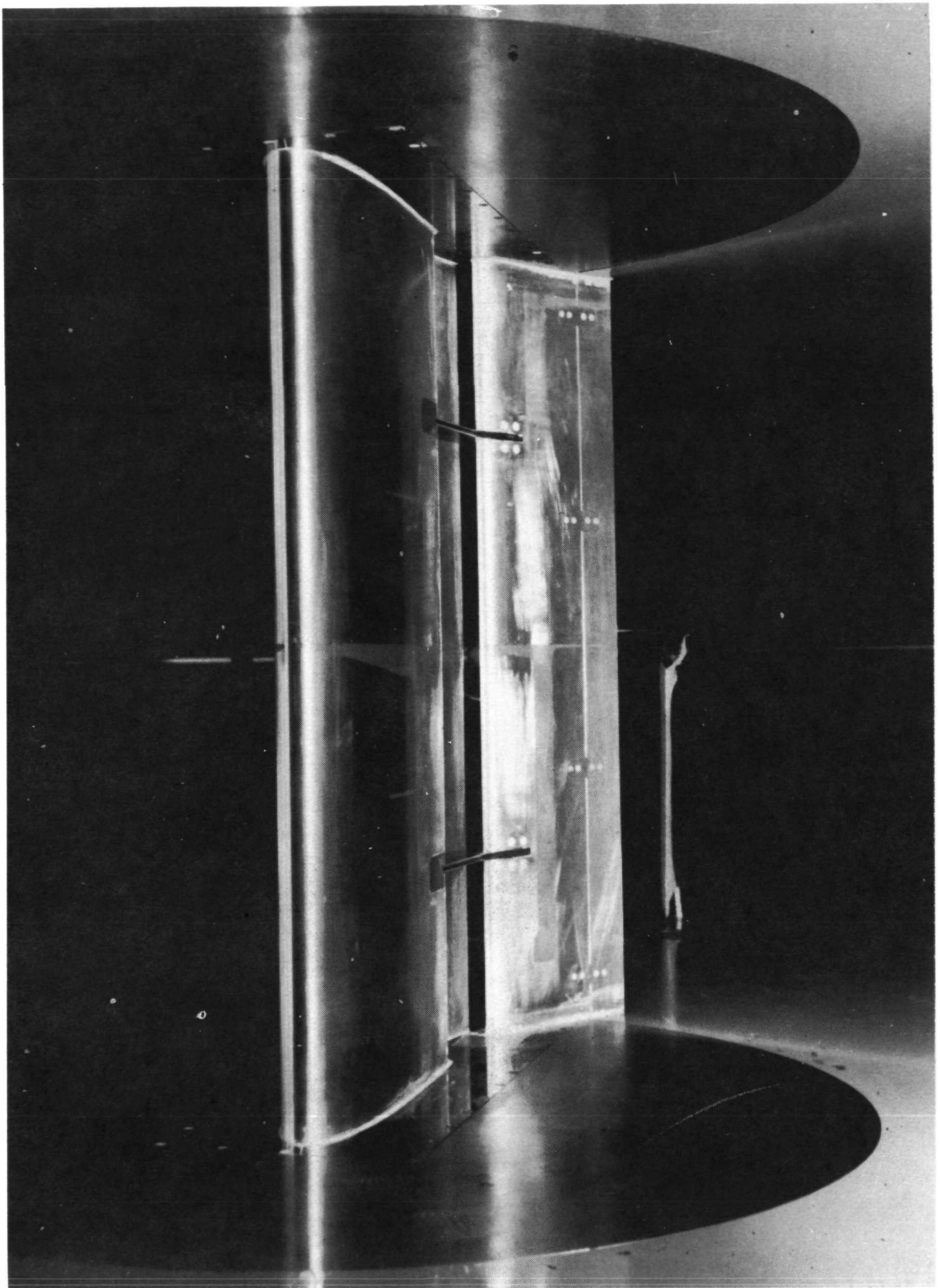
Figure 3.- Model in test section.

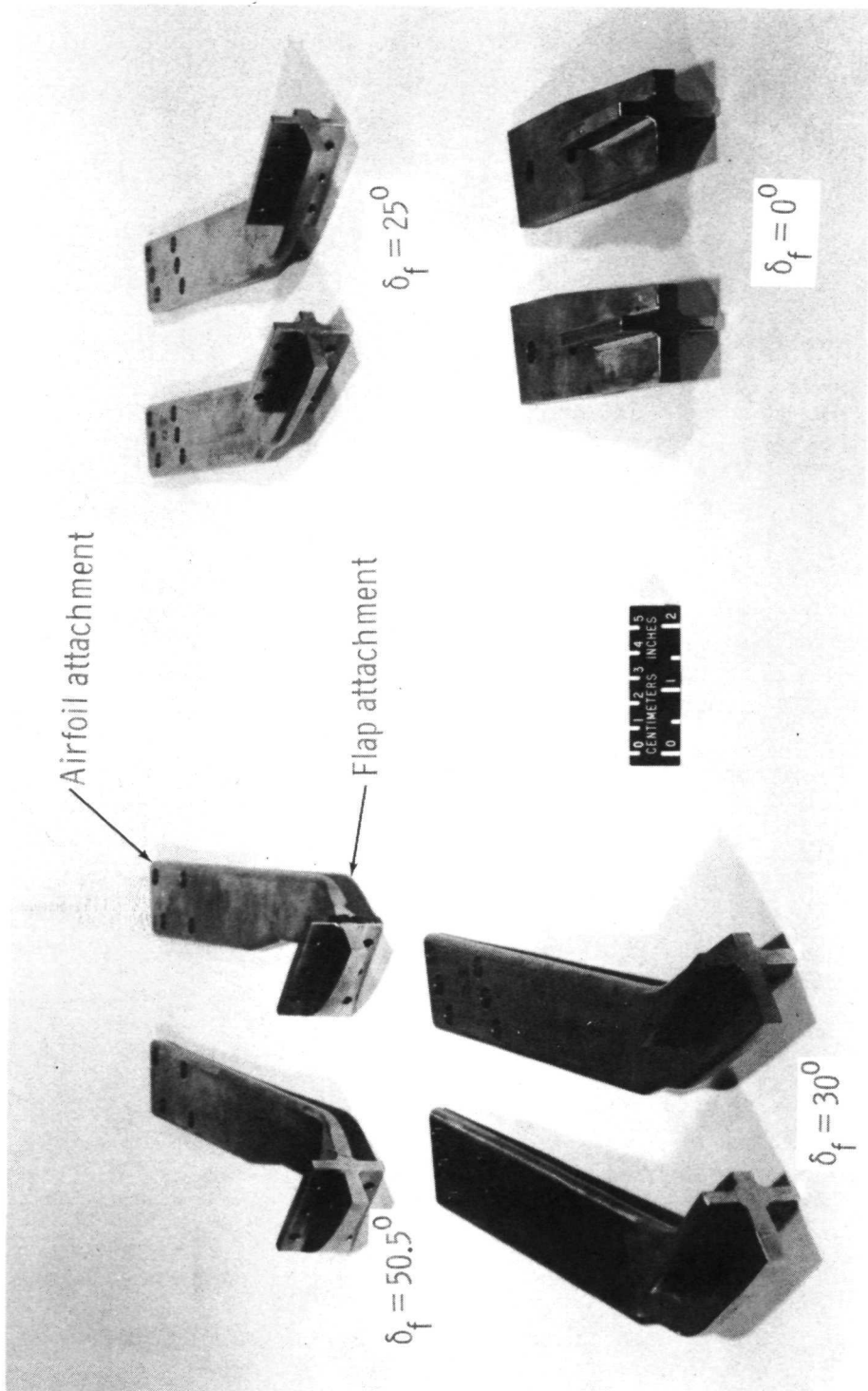


L-71-2560

(b) Front view of lower surface. $\delta_f = 30^\circ$.

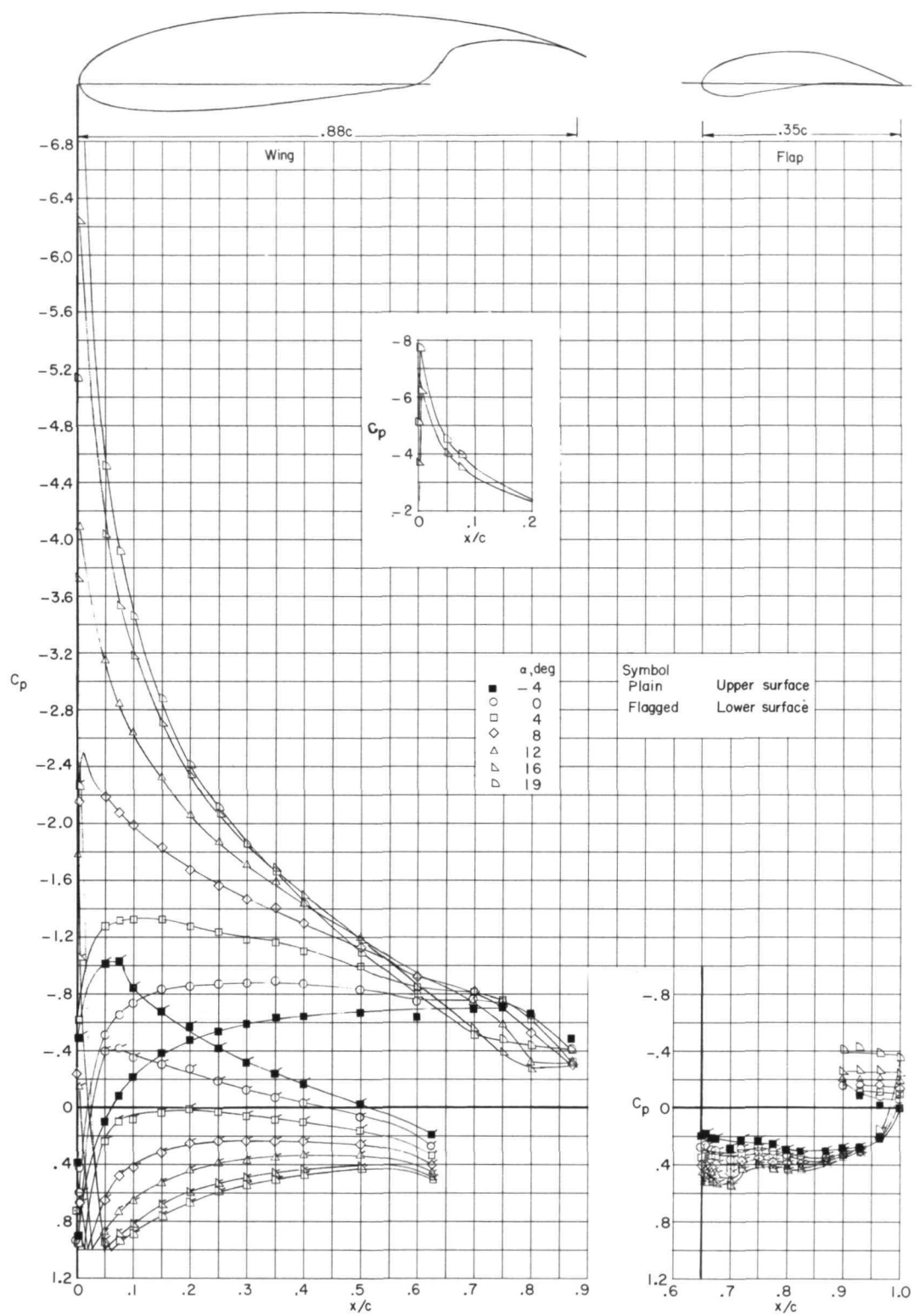
Figure 3.- Concluded.





L-71-3172.1

Figure 4.- Typical flap attachment brackets.



(a) NACA 6716 airfoil; $\delta_f = 0^\circ$.

Figure 5.- Pressure distribution over airfoil section with $0.35c$ single-slotted flap.
Slot entry 1; $R \approx 12 \times 10^6$; $M = 0.23$.

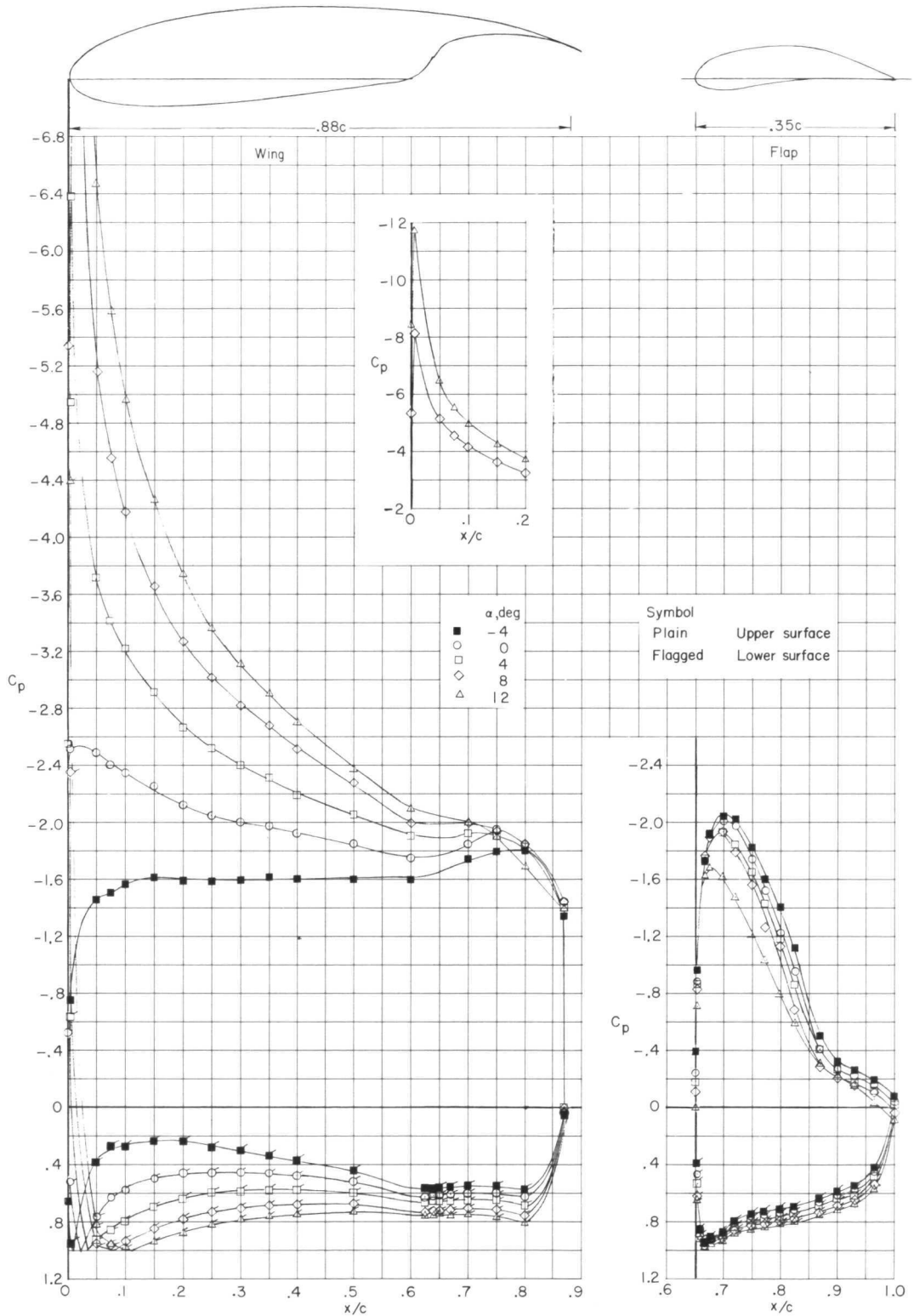
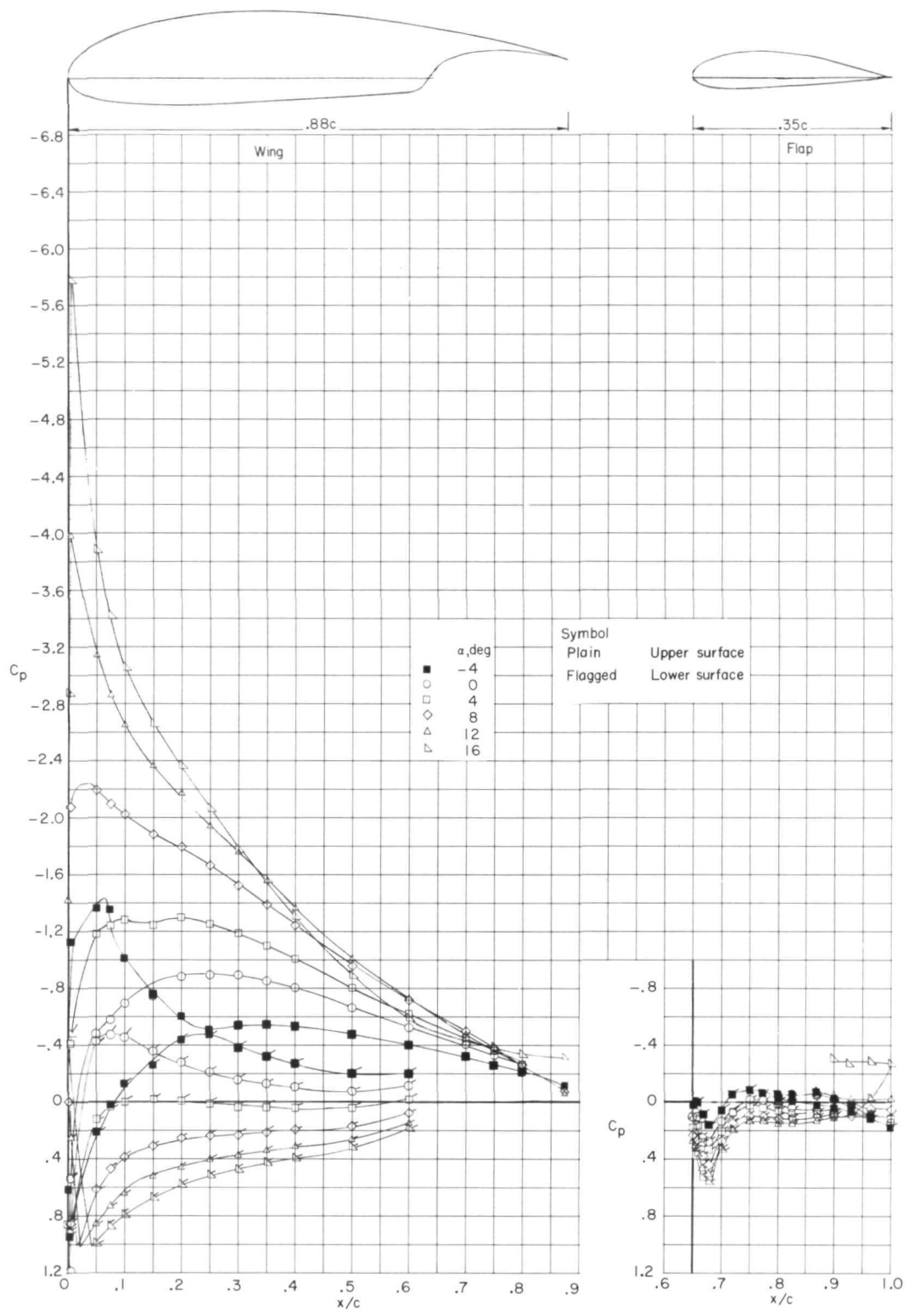
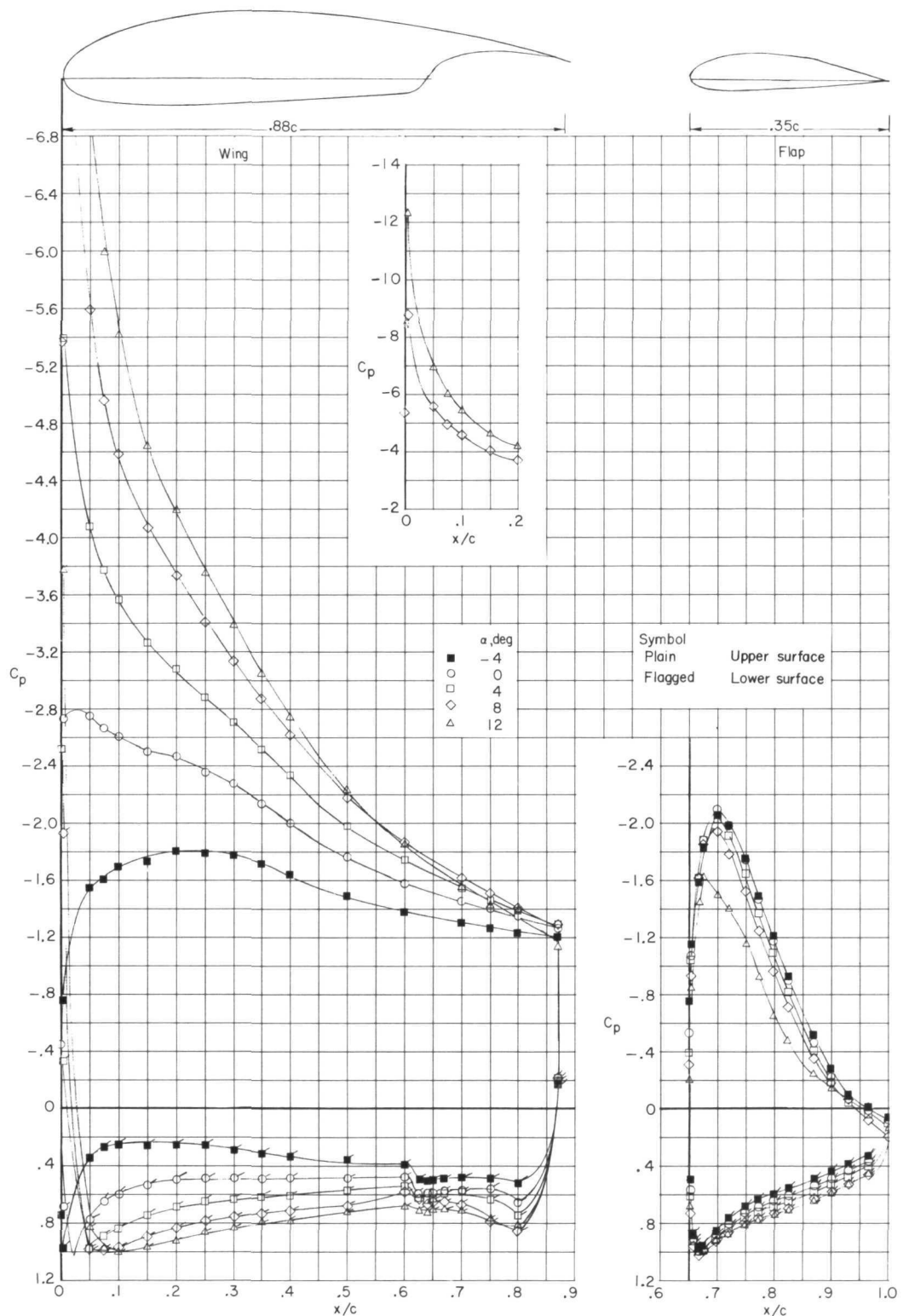


Figure 5.- Continued.



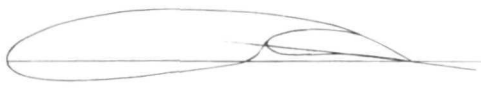
(c) NACA 4416 airfoil; $\delta_f = 0^0$.

Figure 5.- Continued.

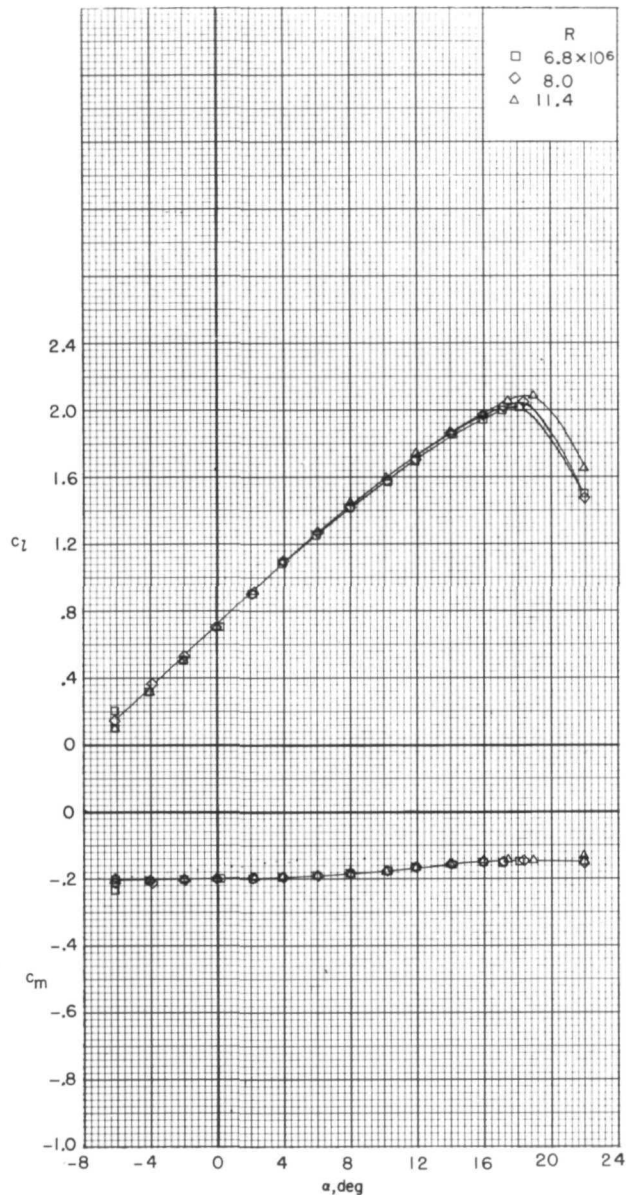


(d) NACA 4416 airfoil; $\delta_f = 30^\circ$; flap leading edge, $x/c = 0.862$; $y/c = 0.007$.

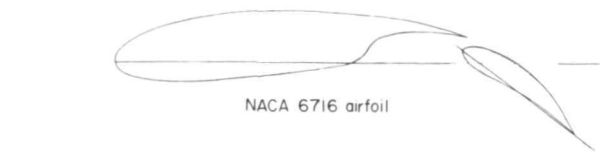
Figure 5.- Concluded.



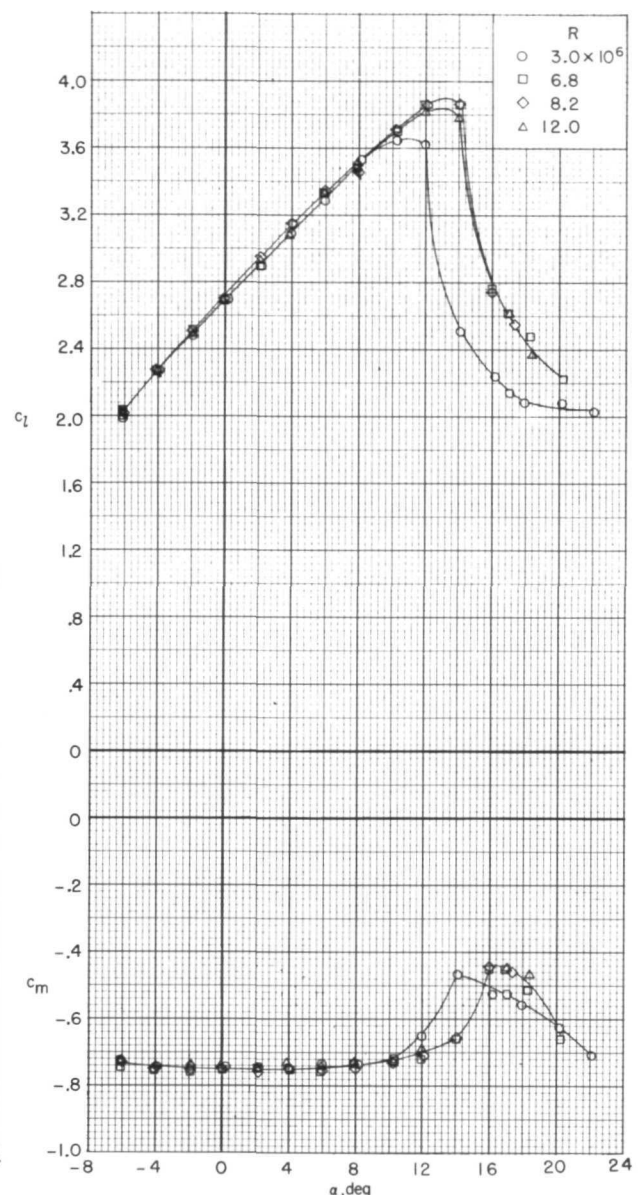
NACA 6716 airfoil



(a) Slot entry 1; $\delta_f = 0^\circ$; $M = 0.23$.

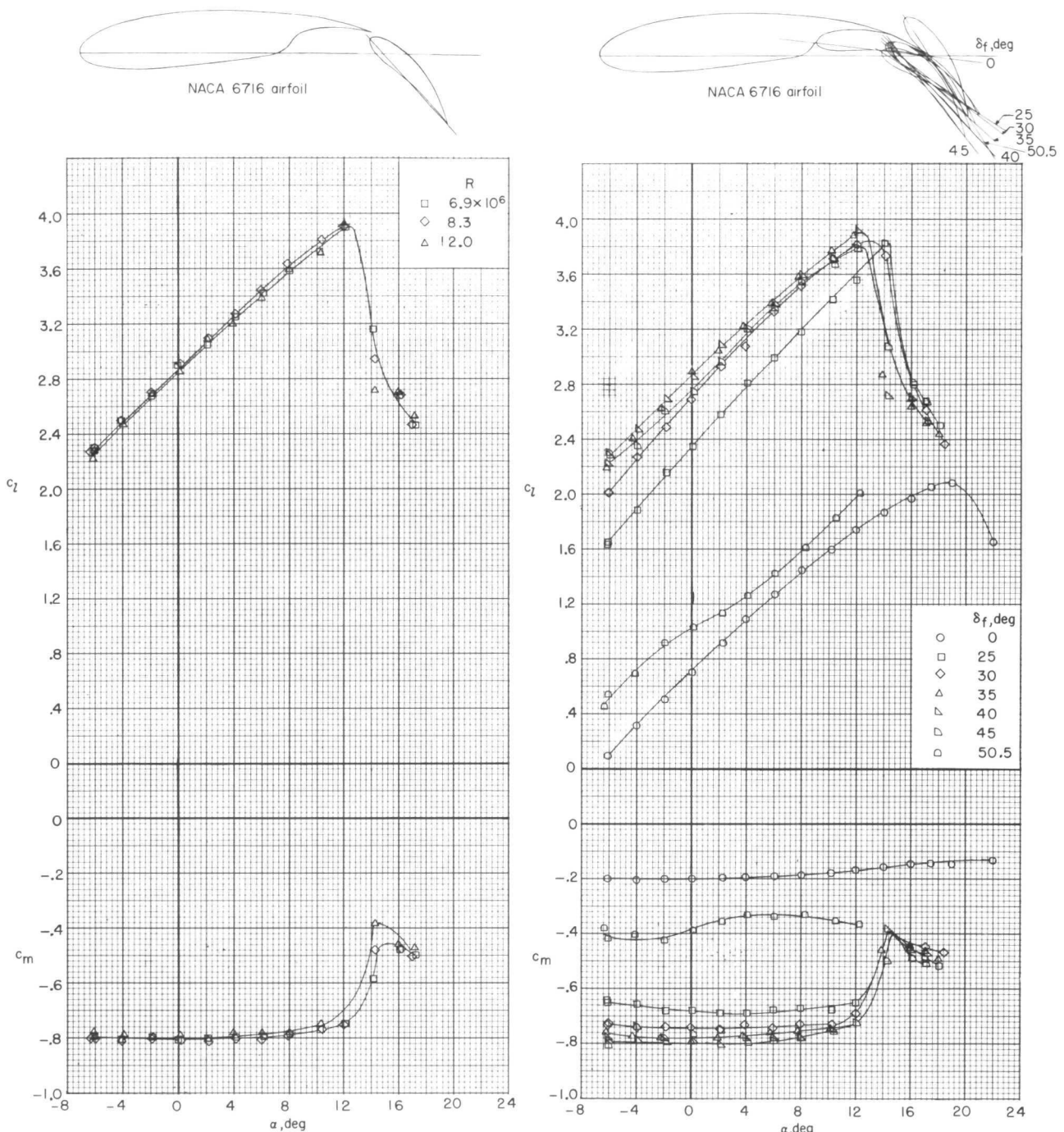


NACA 6716 airfoil



(b) Slot entry 1; $\delta_f = 30^\circ$; $M = 0.23$.

Figure 6.- Lift and pitching-moment characteristics of the NACA 6716 airfoil section with 0.35c single-slotted flap.

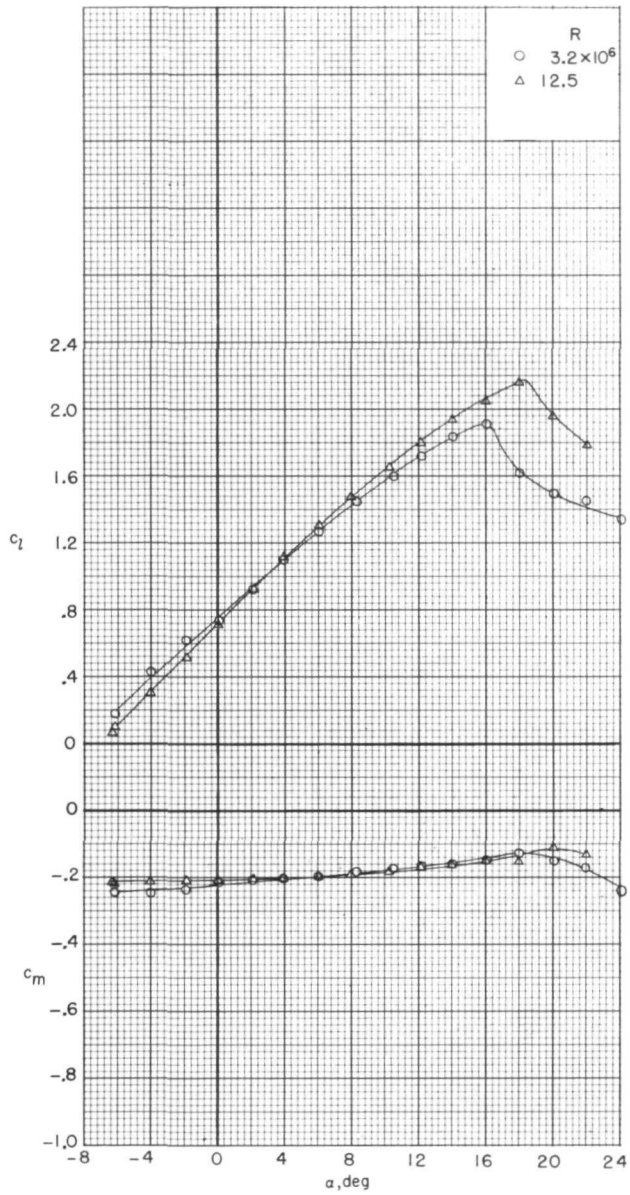




NACA 6716 airfoil



NACA 6716 airfoil



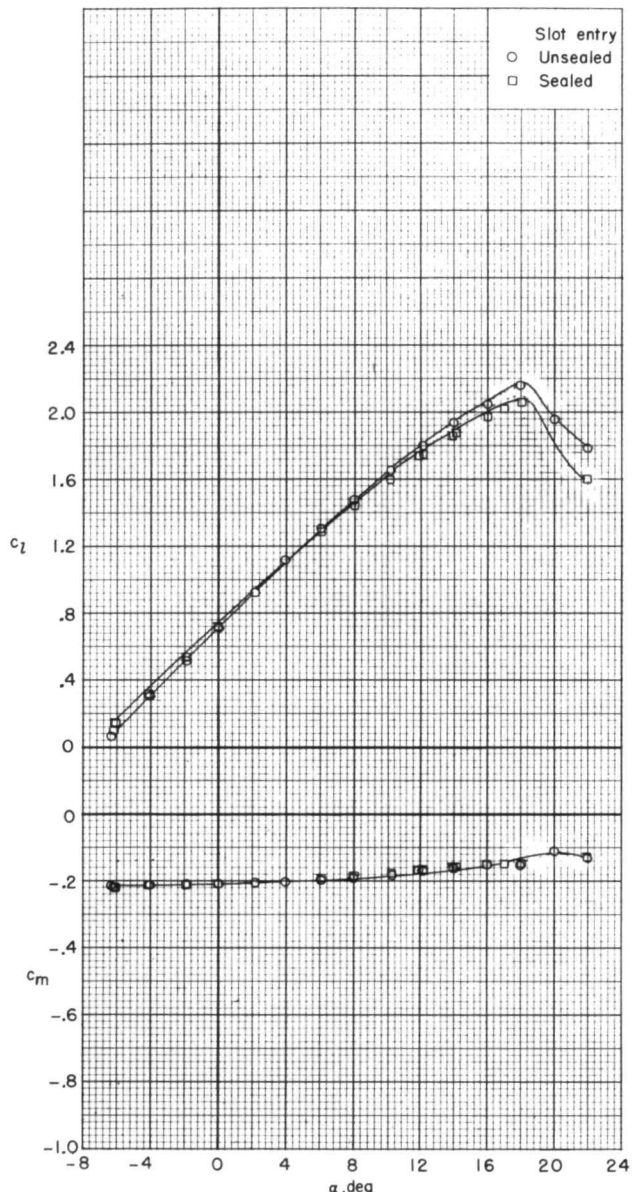
(e) Slot entry 3; $\delta_f = 0^\circ$; $M = 0.23$.

(f) Slot entry 3 sealed; $\delta_f = 0^\circ$; $M = 0.23$.

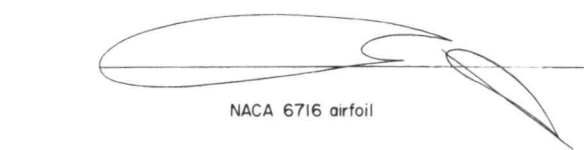
Figure 6.- Continued.



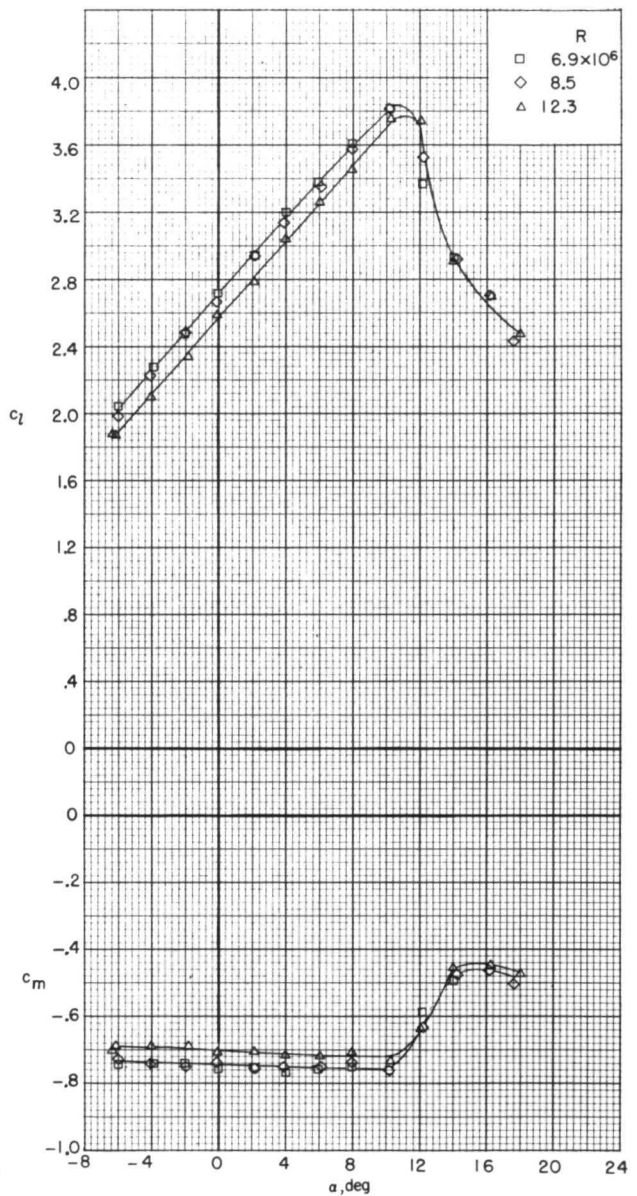
NACA 6716 airfoil



(g) Slot entry 3; $R \approx 12 \times 10^6$; $M = 0.23$.

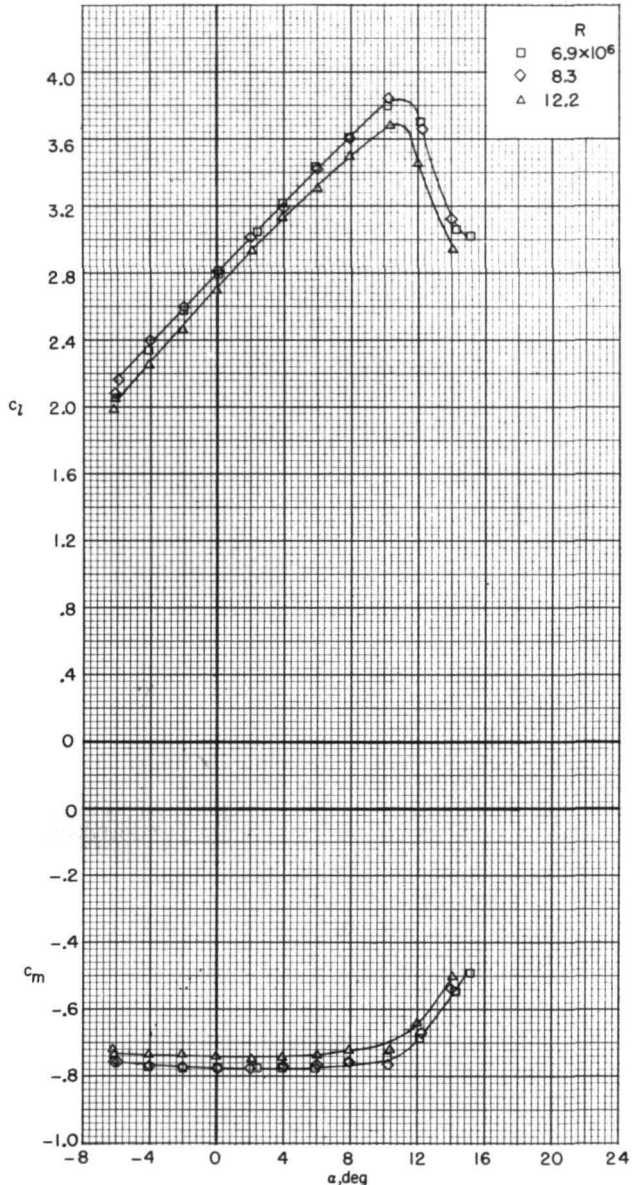
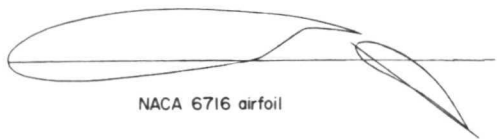


NACA 6716 airfoil

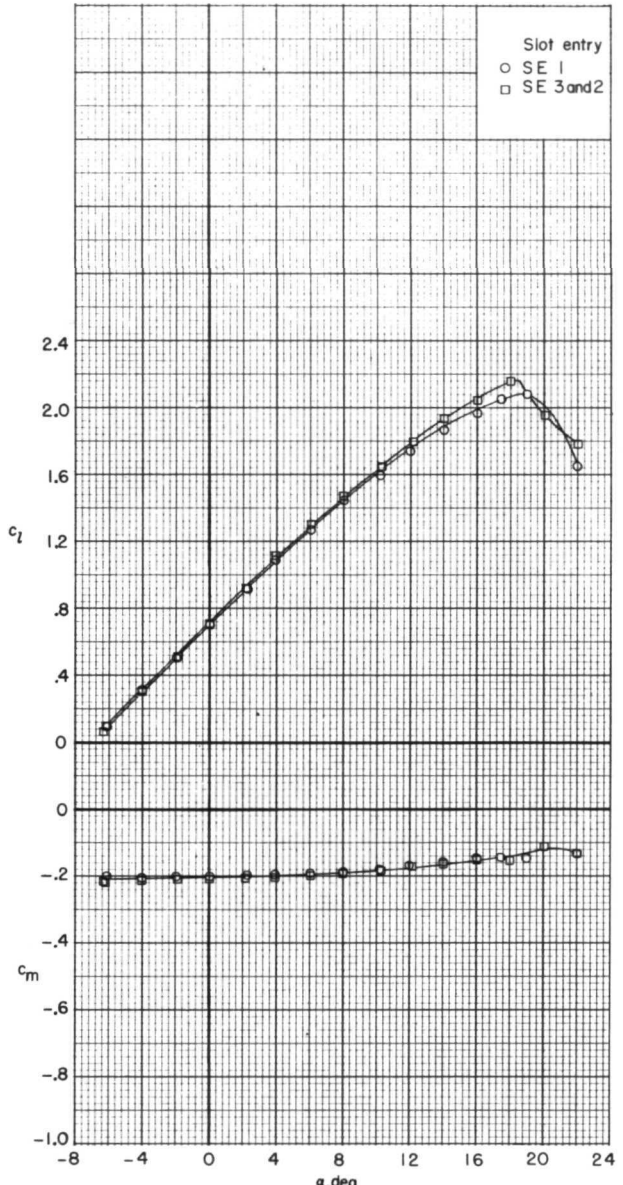
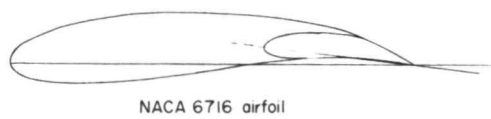


(h) Slot entry 3; $\delta_f = 30^\circ$; $M = 0.23$.

Figure 6.- Continued.

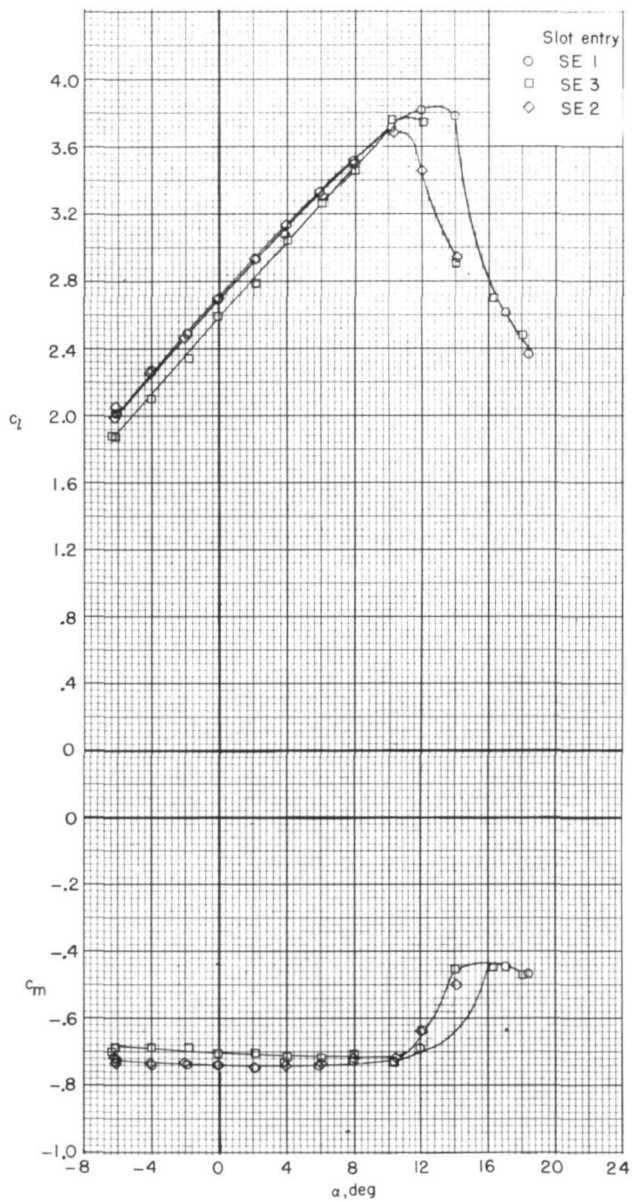
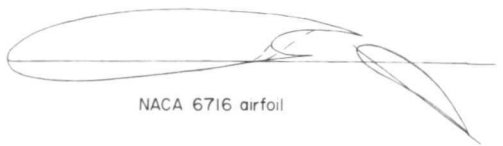


(i) Slot entry 2; $\delta_f = 30^\circ$; $M = 0.23$.



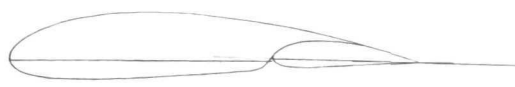
(j) $\delta_f = 0^\circ$; $R \approx 12 \times 10^6$; $M = 0.23$.

Figure 6.- Continued.

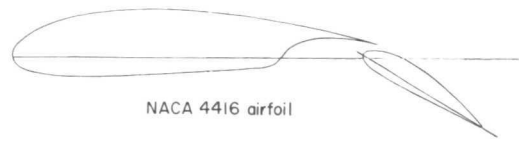


(k) $\delta_f = 30^\circ$; $R \approx 12 \times 10^6$; $M = 0.23$. (l) Slot entry 3 sealed; $\delta_f = 0^\circ$; $R \approx 7 \times 10^6$.

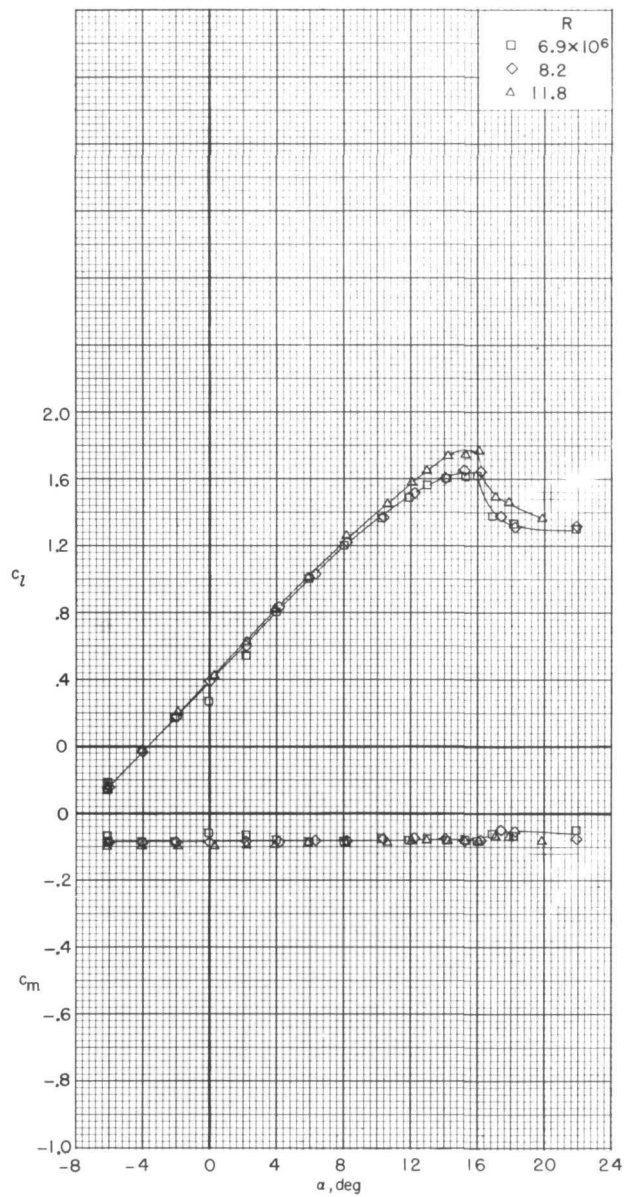
Figure 6.- Concluded.



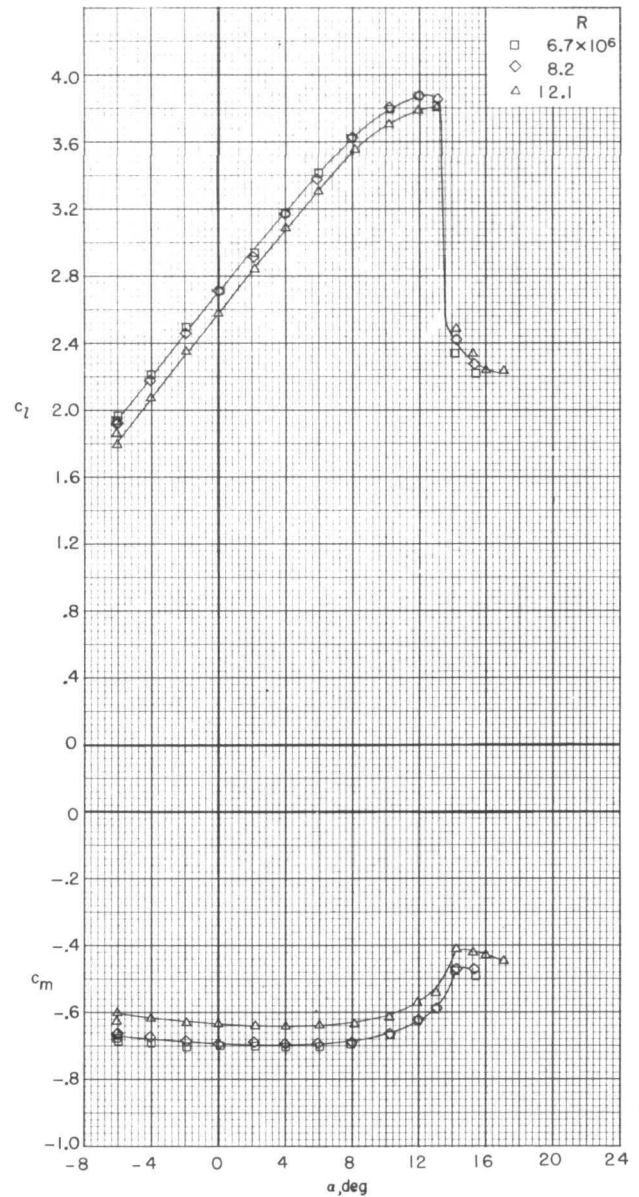
NACA 4416 airfoil



NACA 4416 airfoil



(a) Slot entry 1; $\delta_f = 0^\circ$.



(b) Slot entry 1; $\delta_f = 30^\circ$.

Figure 7.- Lift and pitching-moment characteristics of NACA 4416 airfoil section with 0.35c single-slotted flap. $M = 0.23$.

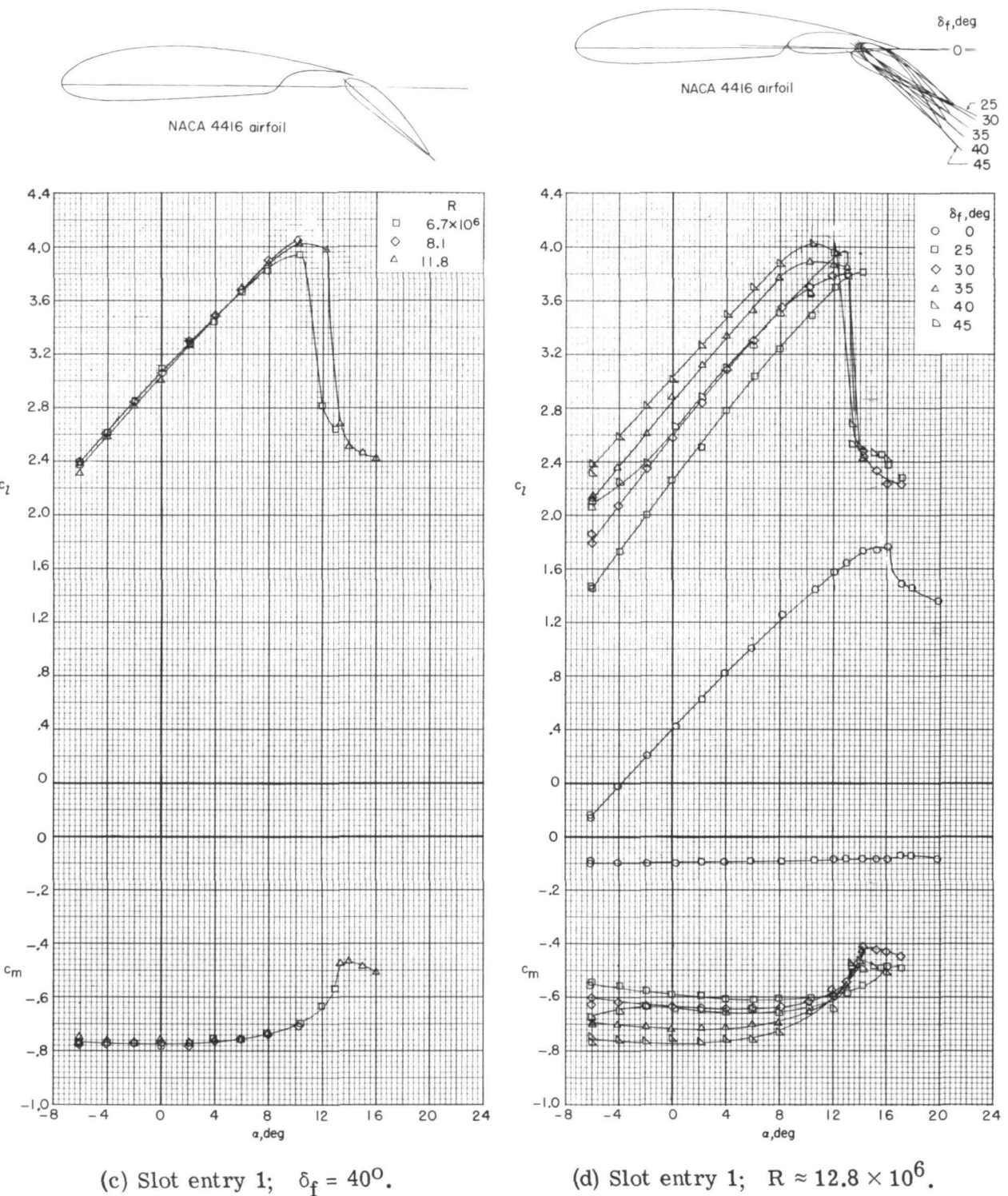
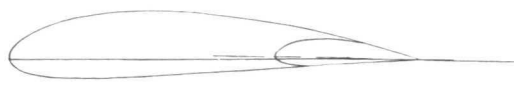
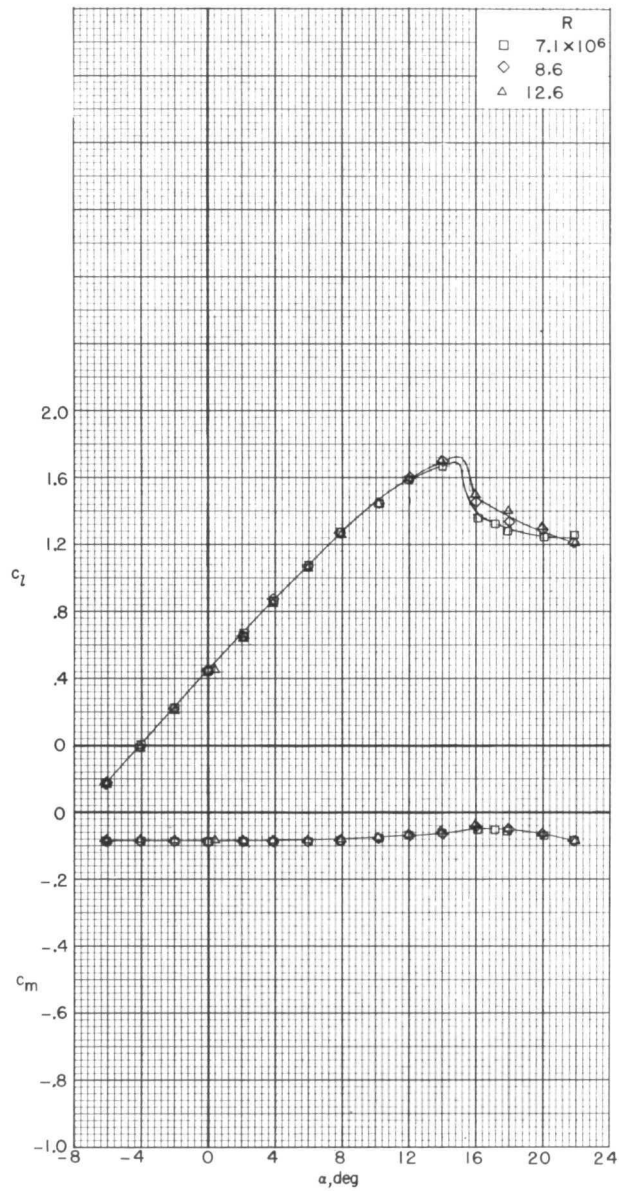


Figure 7.- Continued.



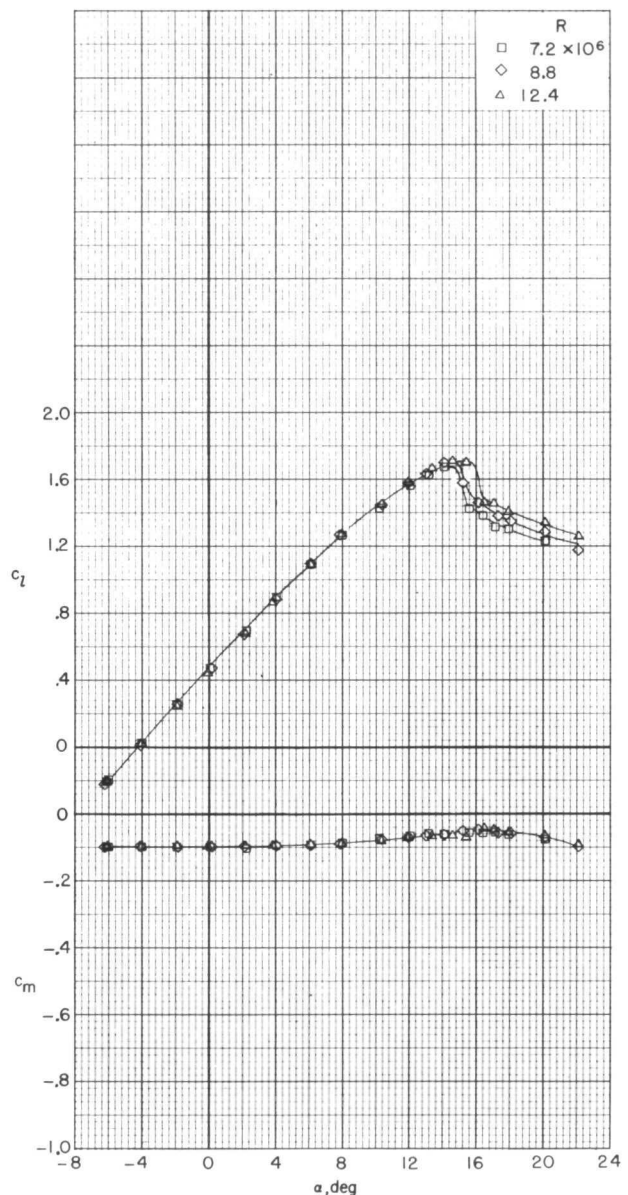
NACA 4416 airfoil



(e) Slot entry 3; $\delta_f = 0^\circ$.



NACA 4416 airfoil

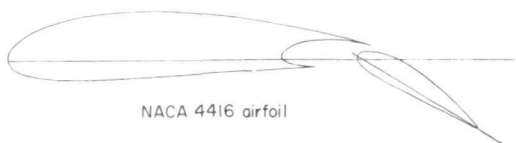


(f) Slot entry 3 sealed; $\delta_f = 0^\circ$.

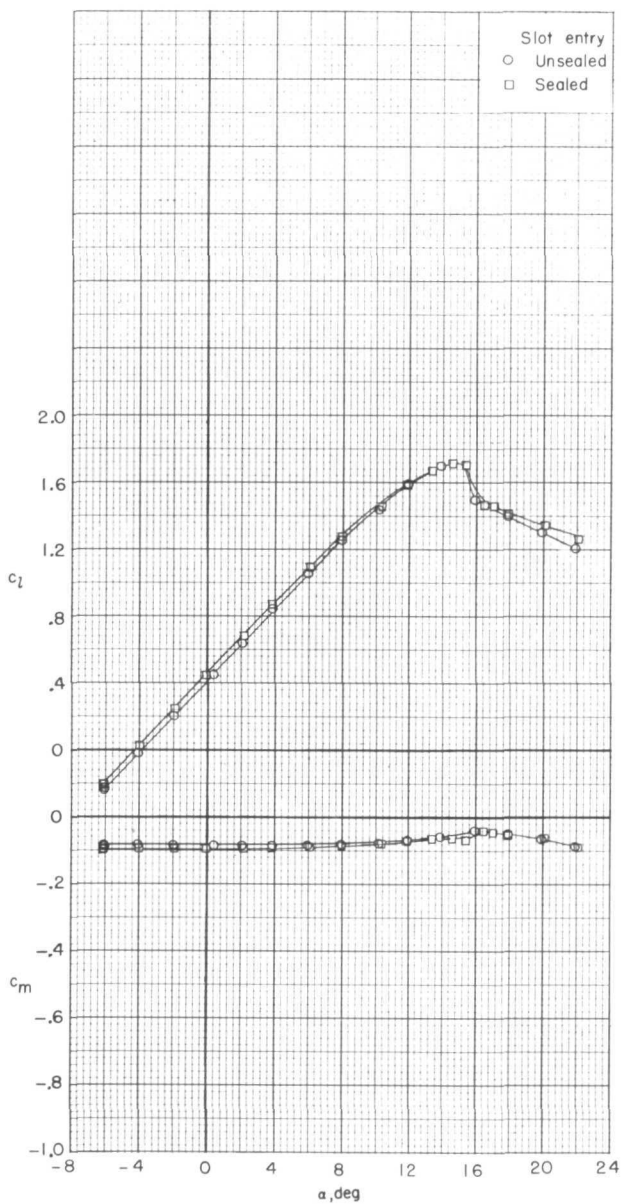
Figure 7.- Continued.



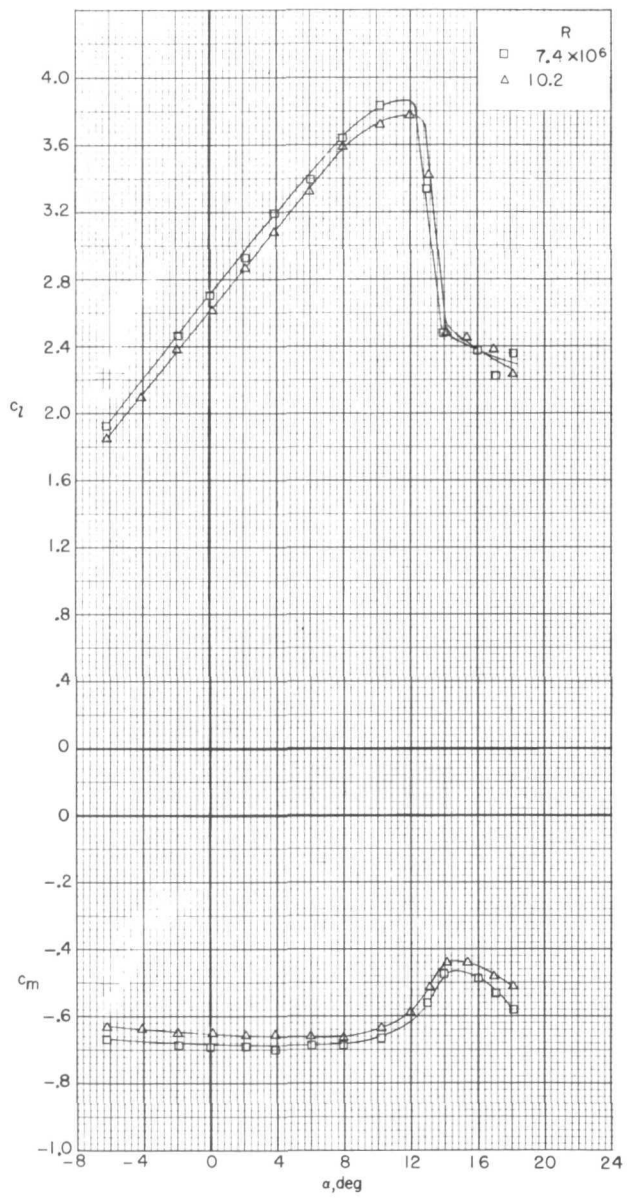
NACA 4416 airfoil



NACA 4416 airfoil

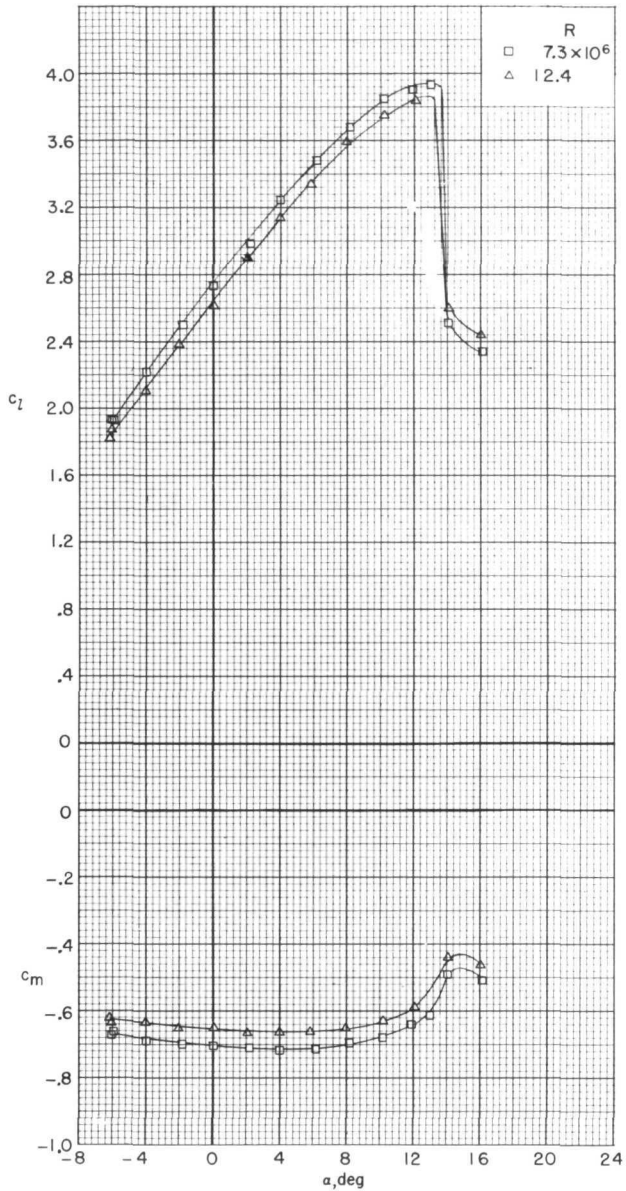
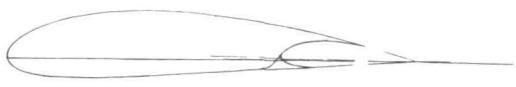
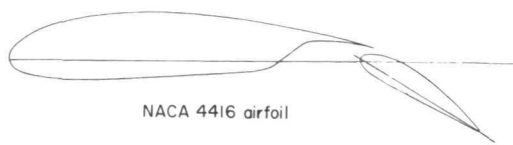


(g) Slot entry 3; $\delta_f = 0^\circ$; $R \approx 12 \times 10^6$.

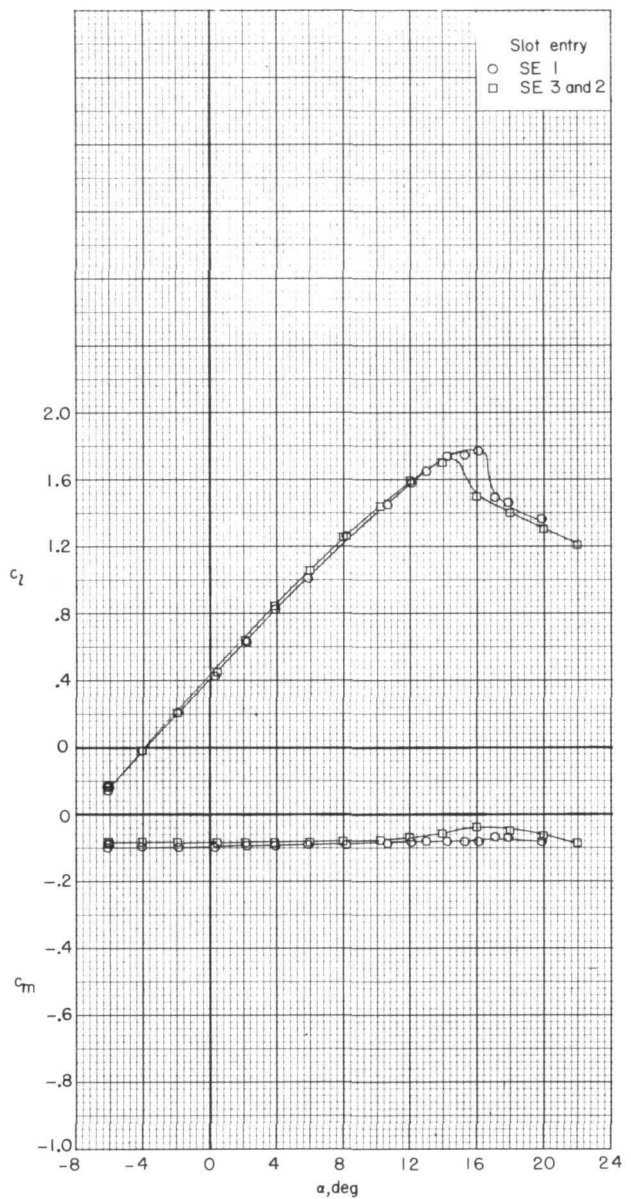


(h) Slot entry 3; $\delta_f = 30^\circ$.

Figure 7.- Continued.

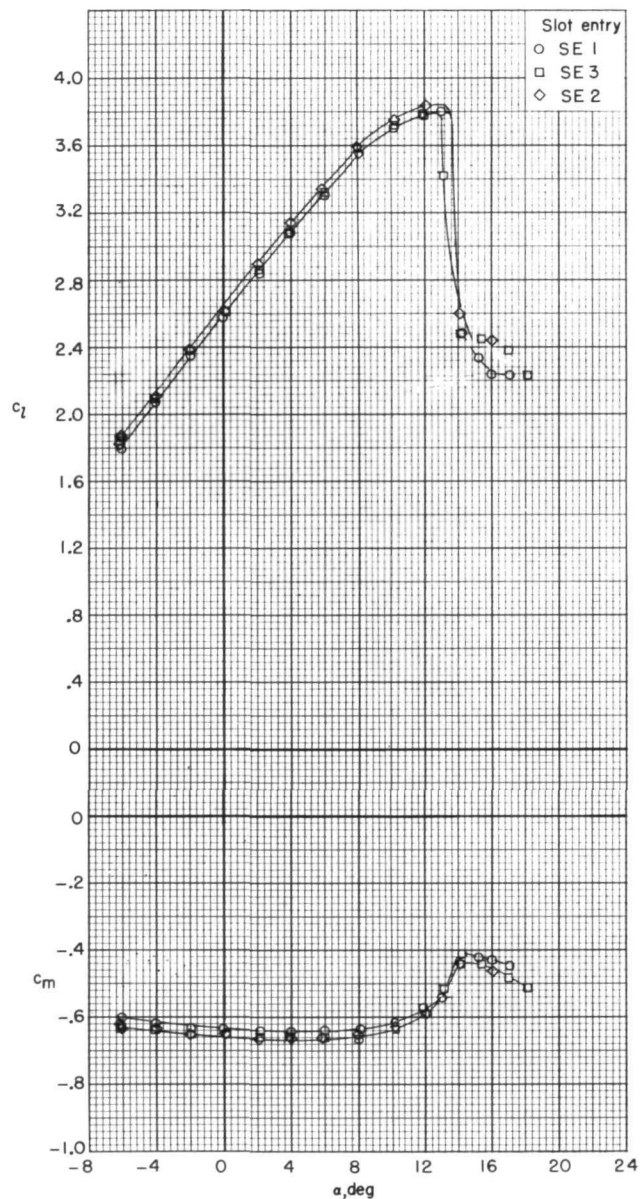
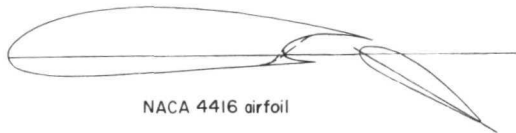


(i) Slot entry 2; $\delta_f = 30^\circ$.

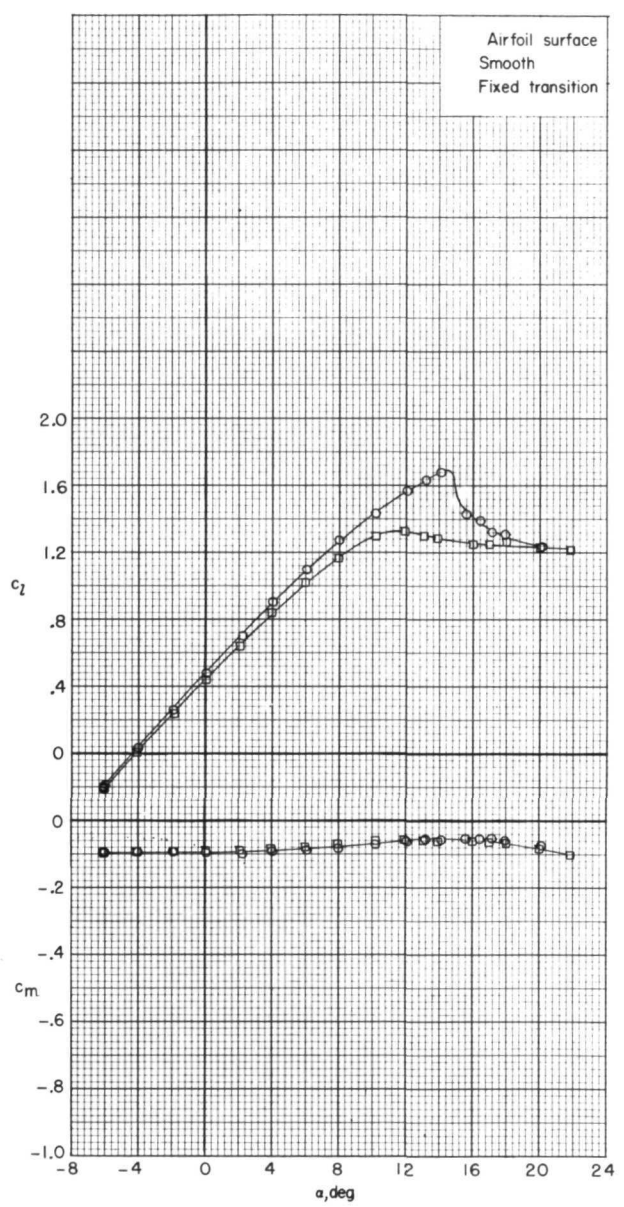
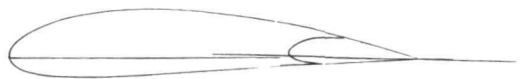


(j) $\delta_f = 0^\circ$; $R \approx 12 \times 10^6$.

Figure 7.- Continued.

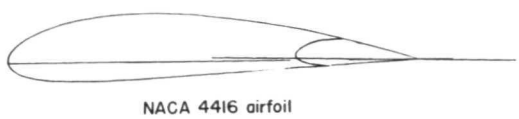


(k) $\delta_f = 30^\circ$; $R \approx 12 \times 10^6$.

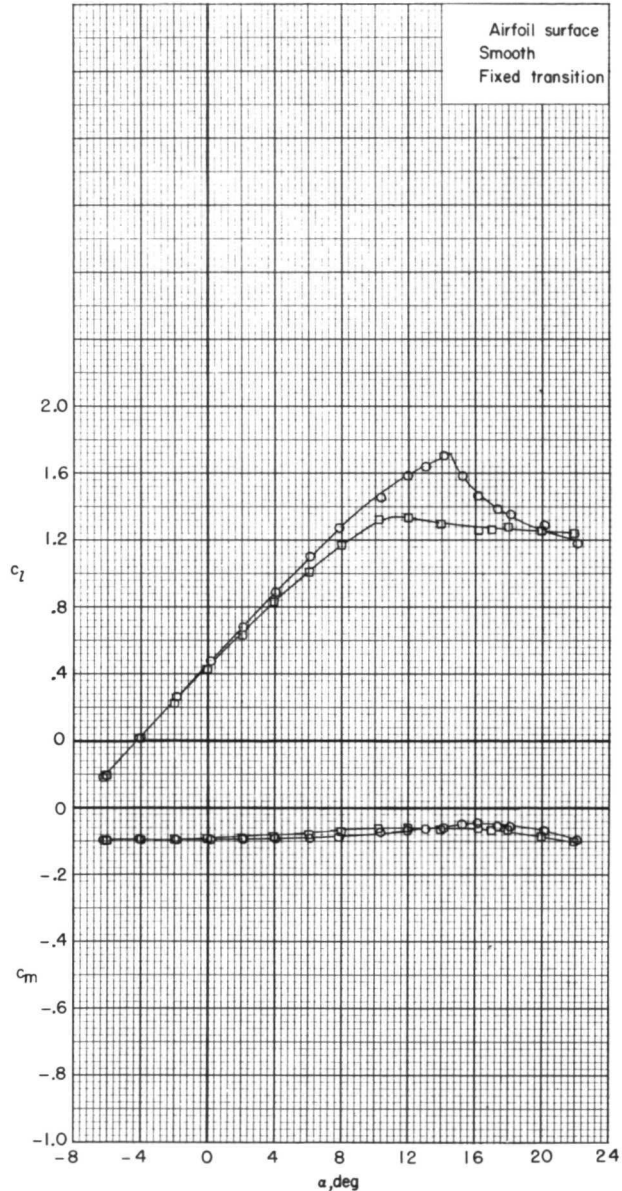


(l) Slot entry 3 sealed; $\delta_f = 0^\circ$; $R \approx 7 \times 10^6$.

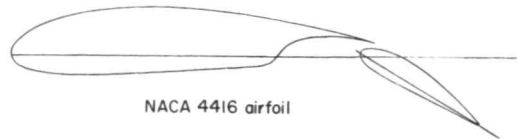
Figure 7.- Continued.



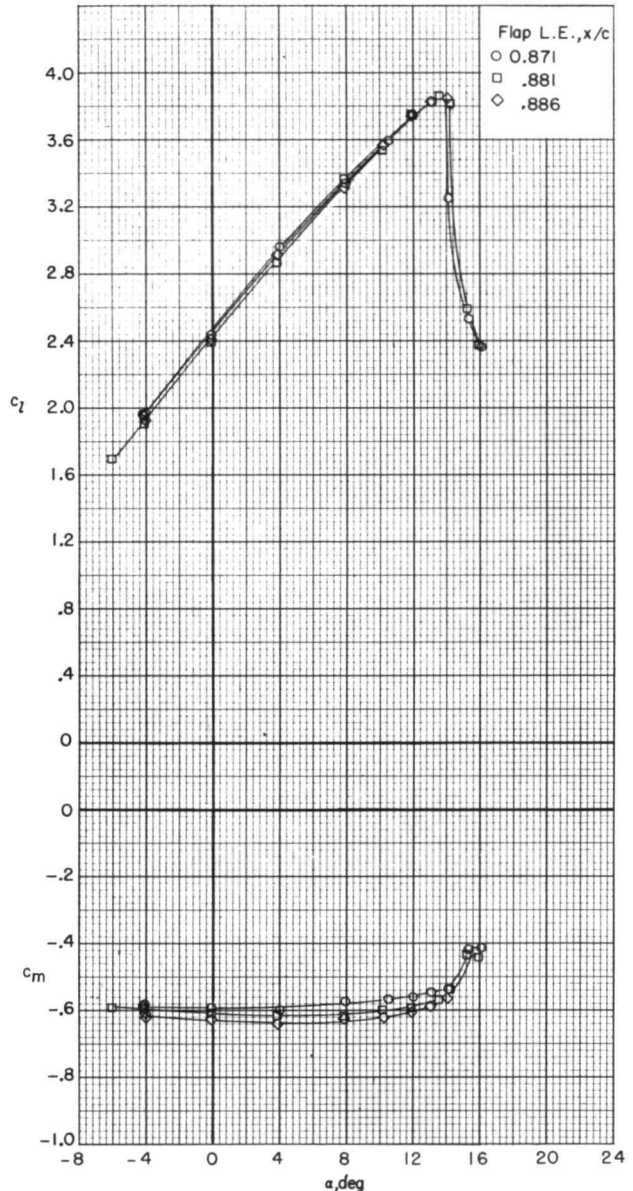
NACA 4416 airfoil



(m) Slot entry 3 sealed; $\delta_f = 0^\circ$;
 $R \approx 9 \times 10^6$.

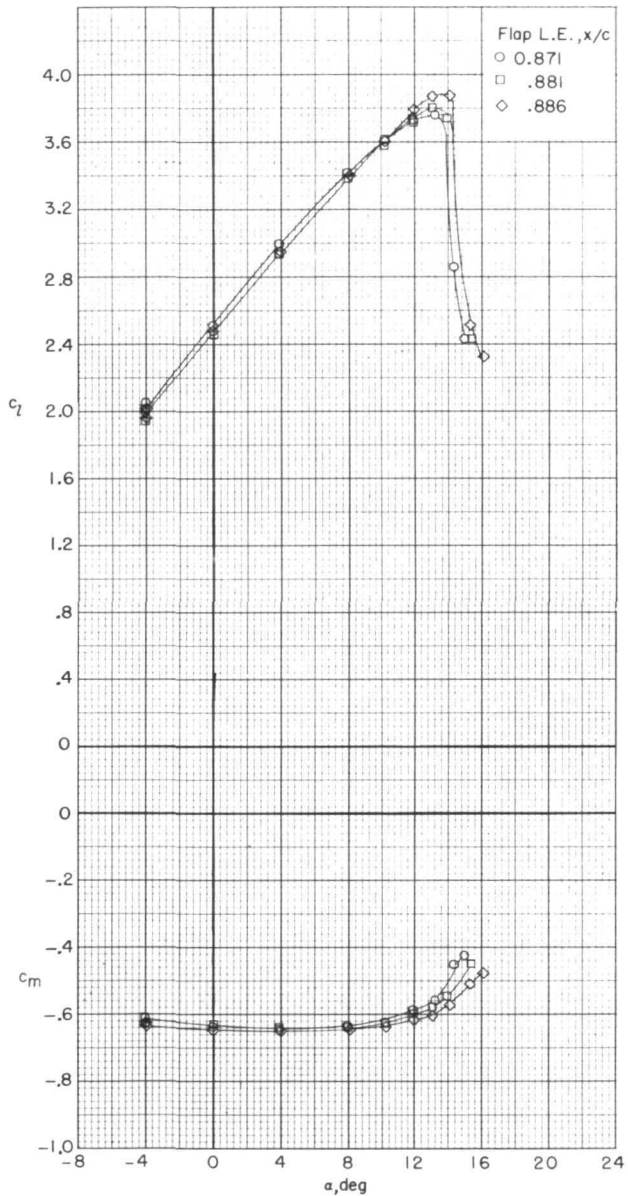
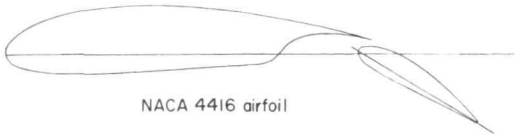


NACA 4416 airfoil

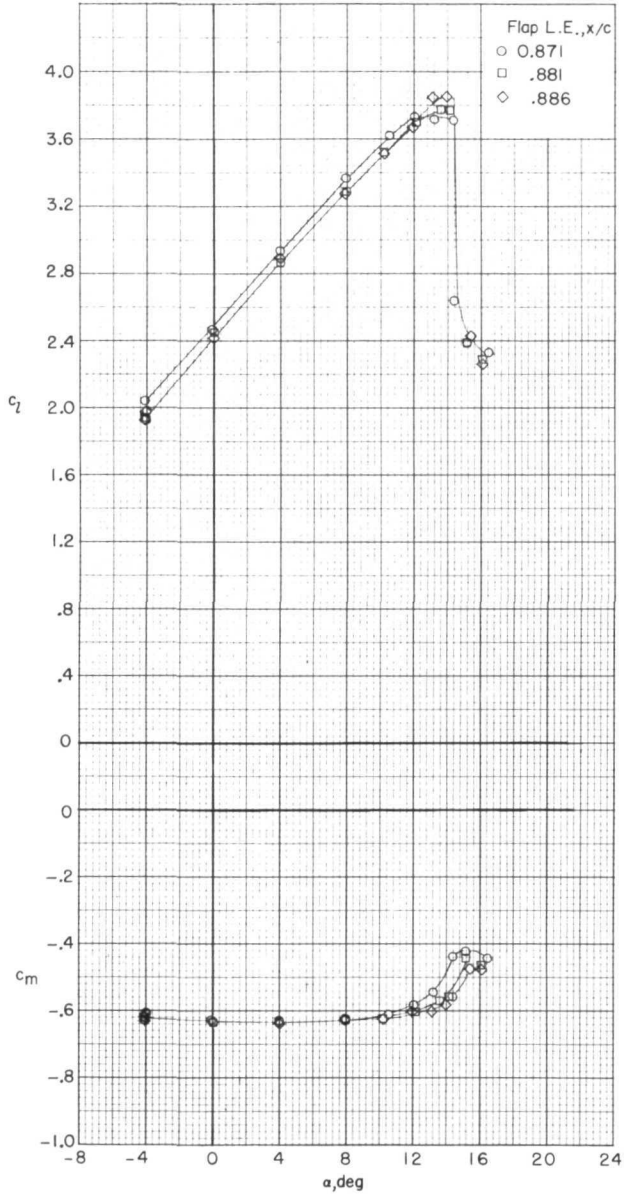


(n) Flap leading-edge matrix position,
 $y/c = 0.015$; slot entry 1; $\delta_f = 30^\circ$;
 $R \approx 12 \times 10^6$.

Figure 7.- Continued.

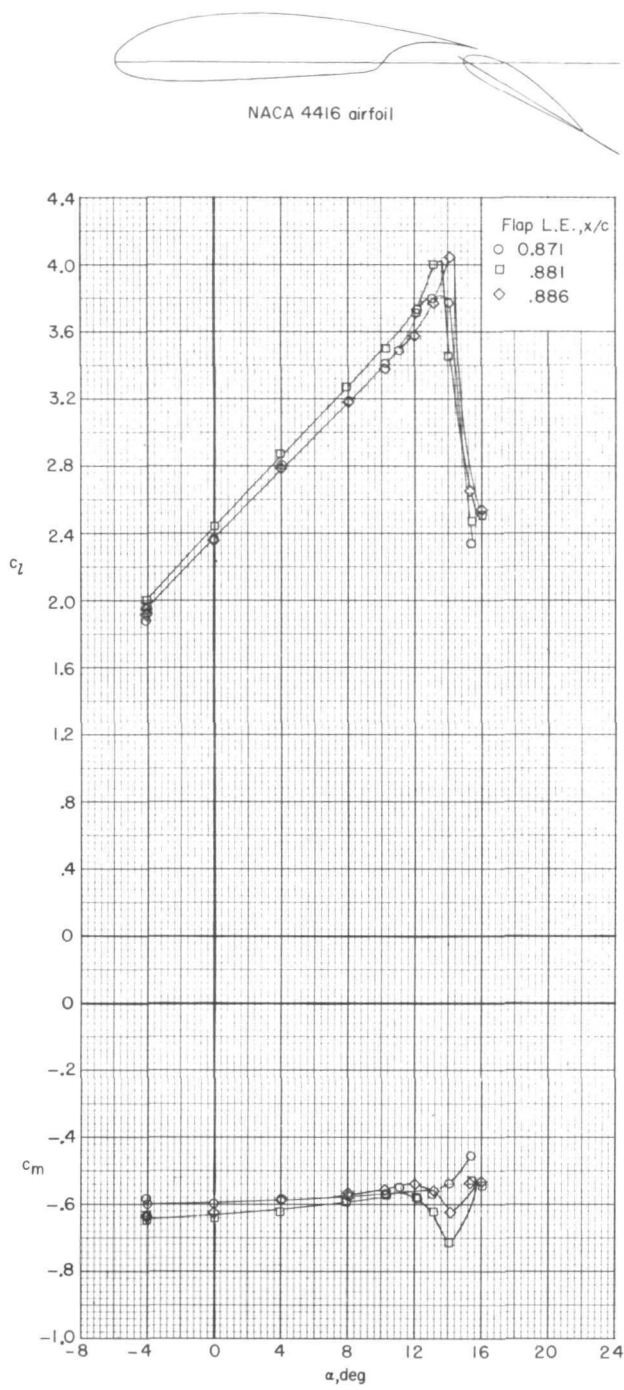


(o) Flap leading-edge matrix position,
 $y/c = 0.010$; slot entry 1; $\delta_f = 30^\circ$;
 $R \approx 12 \times 10^6$.



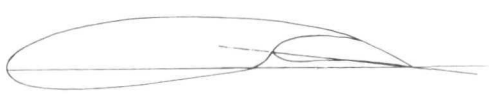
(p) Flap leading-edge matrix position,
 $y/c = 0.005$; slot entry 1; $\delta_f = 30^\circ$;
 $R \approx 12 \times 10^6$.

Figure 7.- Continued.

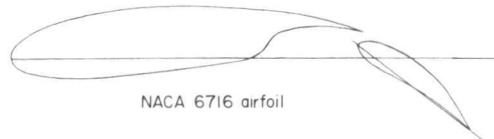


(q) Flap leading-edge matrix position, $y/c = -0.005$;
 slot entry 1; $\delta_f = 30^\circ$; $R \approx 12 \times 10^6$.

Figure 7.- Concluded.



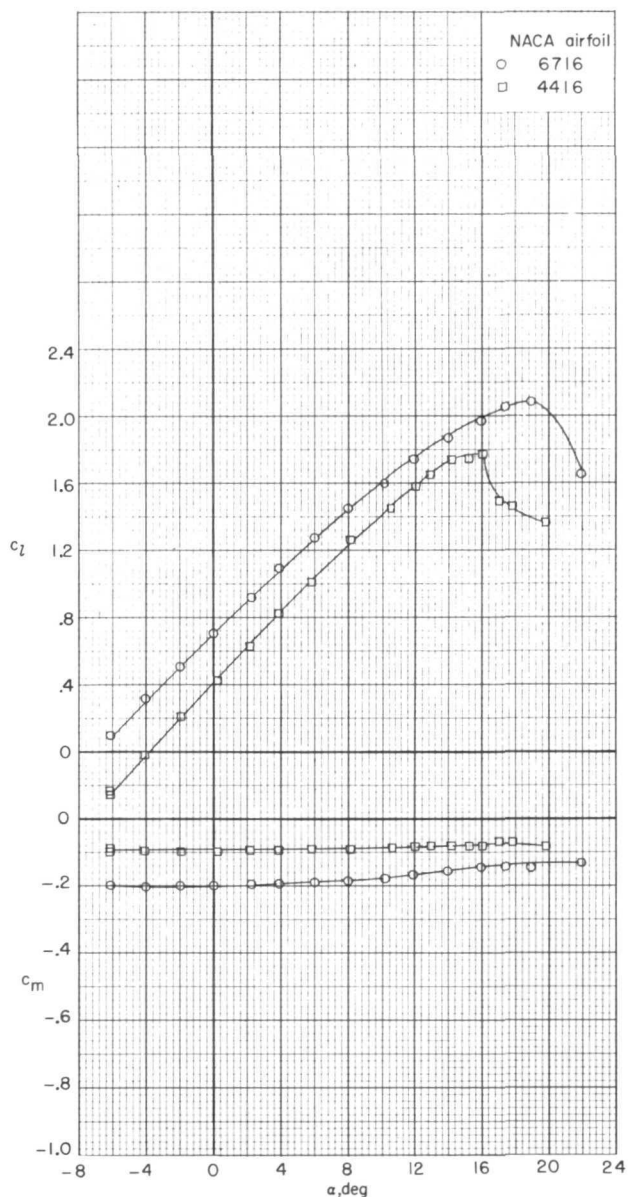
NACA 6716 airfoil



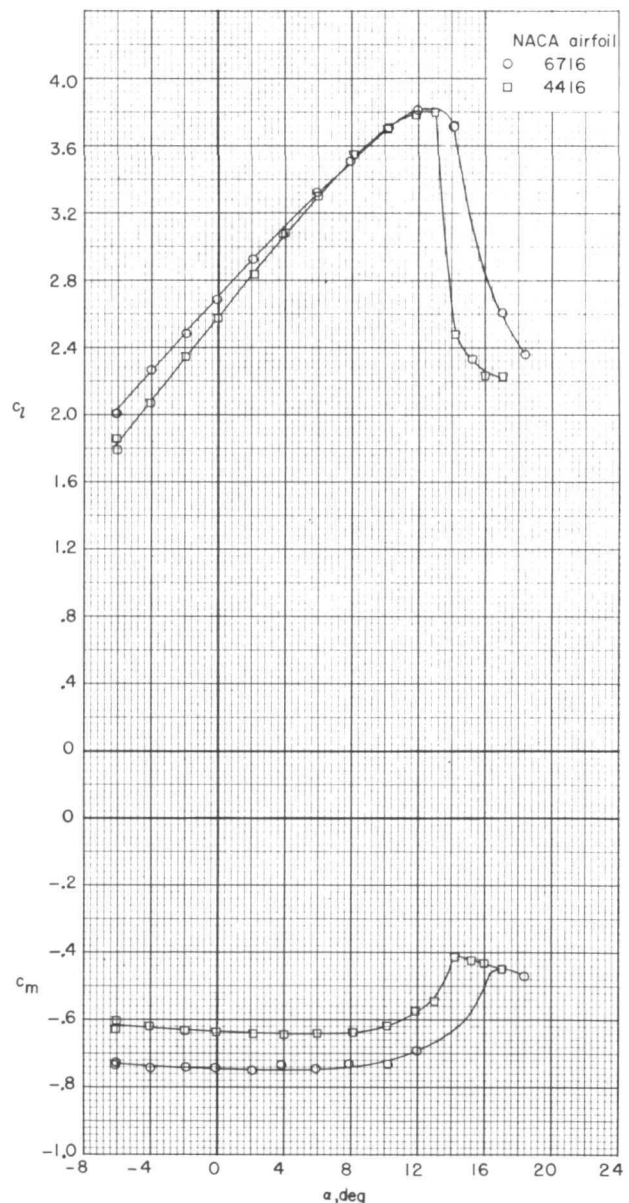
NACA 6716 airfoil



NACA 4416 airfoil



(a) Slot entry 1; $\delta_f = 0^\circ$.



(b) Slot entry 1; $\delta_f = 30^\circ$.

Figure 8.- Lift and pitching-moment characteristics of NACA 6716 and NACA 4416 airfoils. $R \approx 12 \times 10^6$; $M = 0.23$.

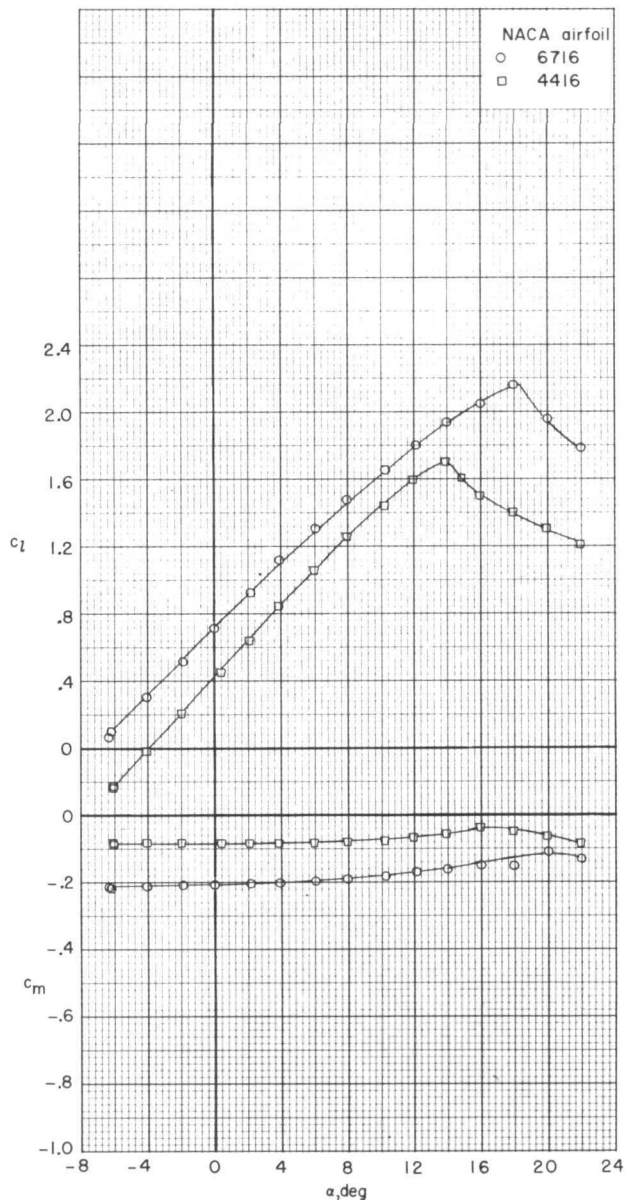
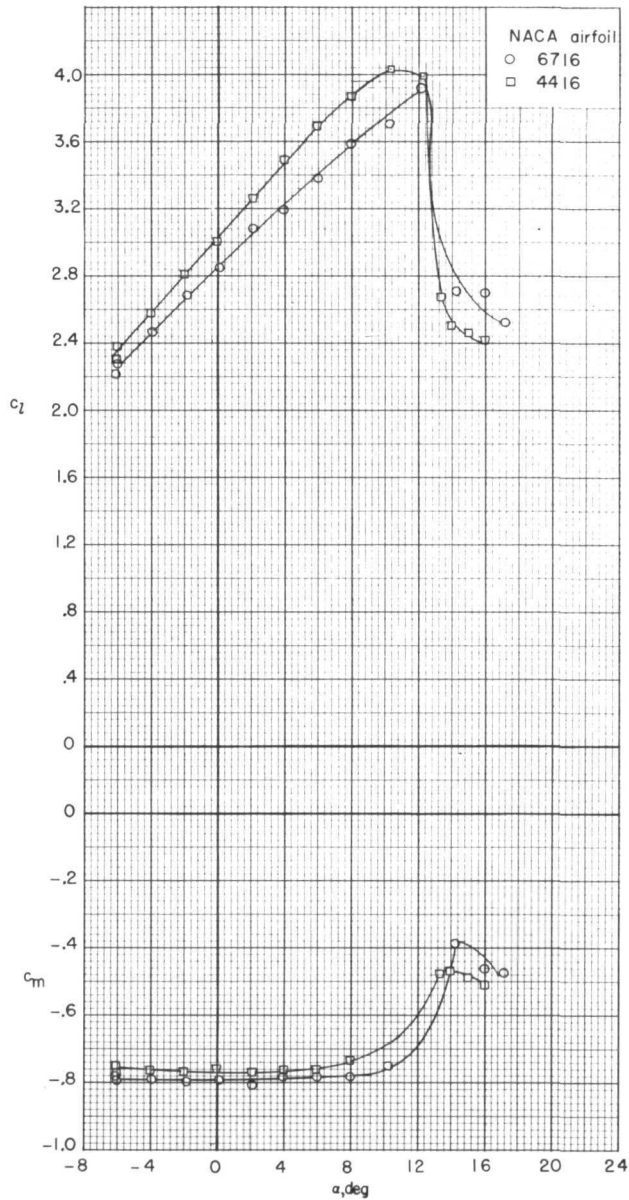
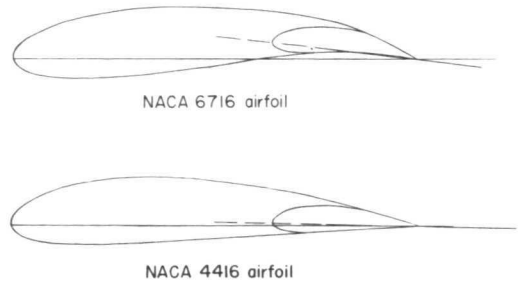
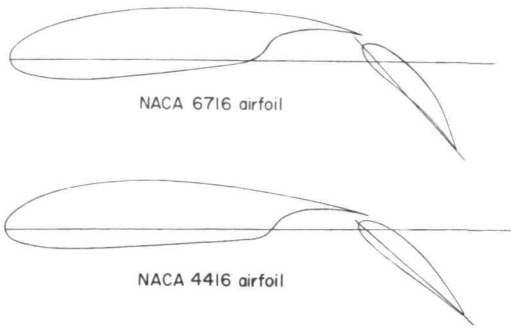
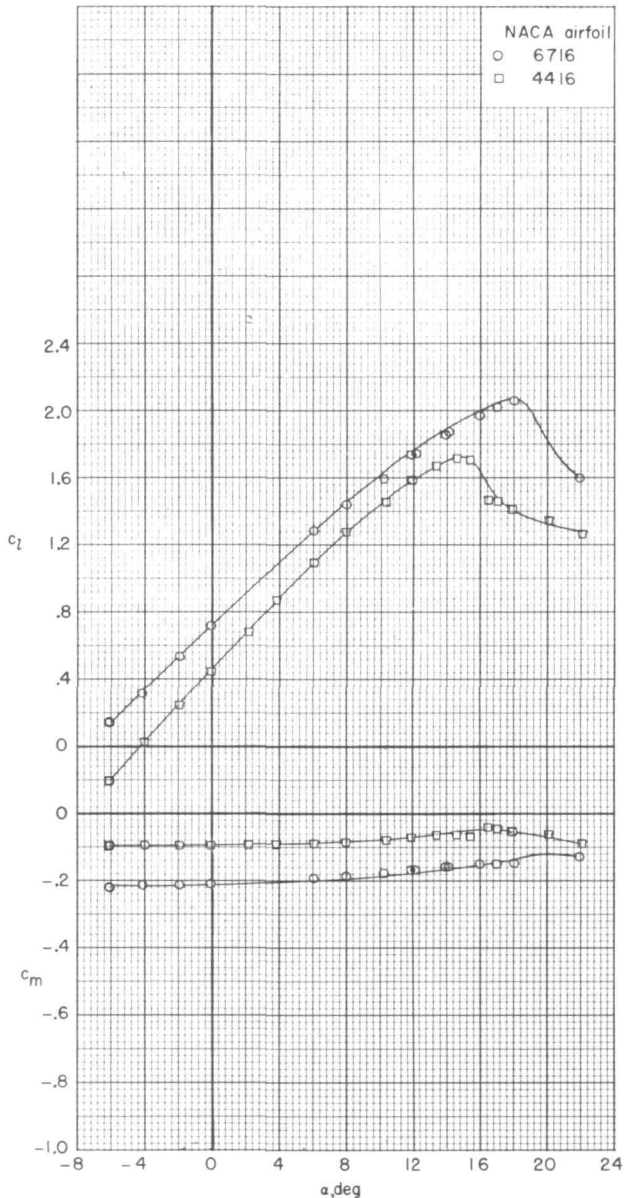
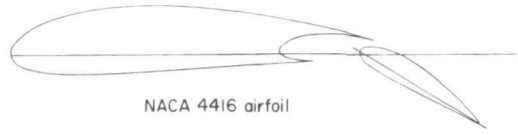
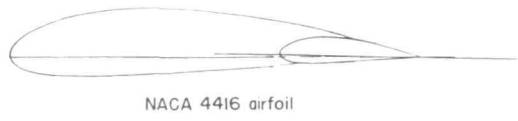
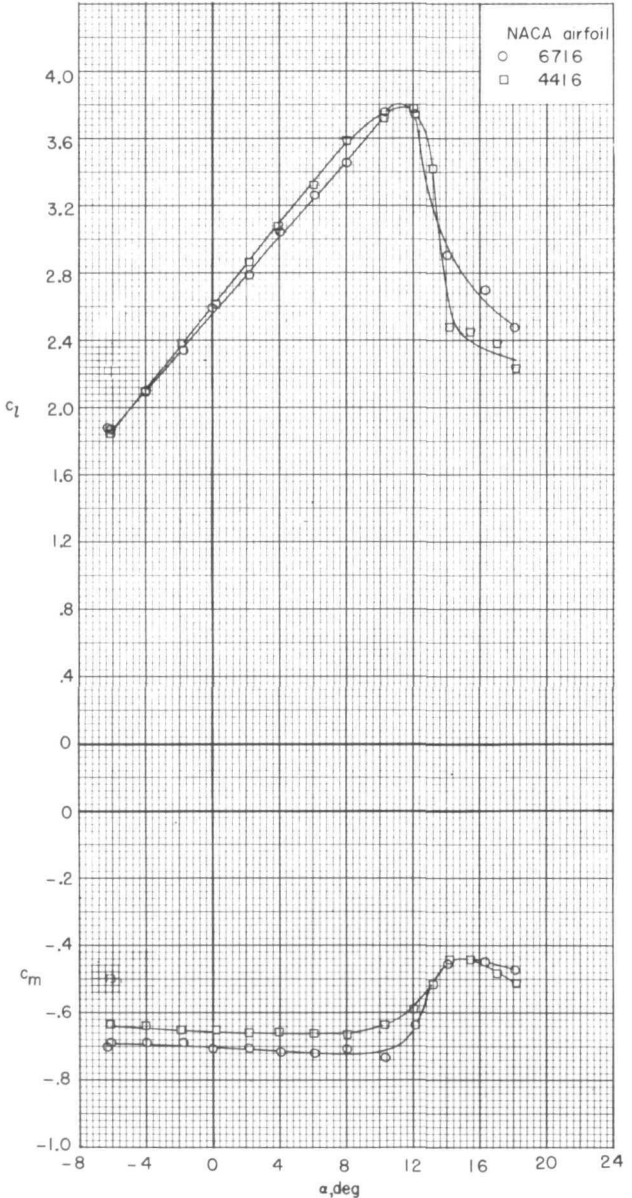


Figure 8.- Continued.

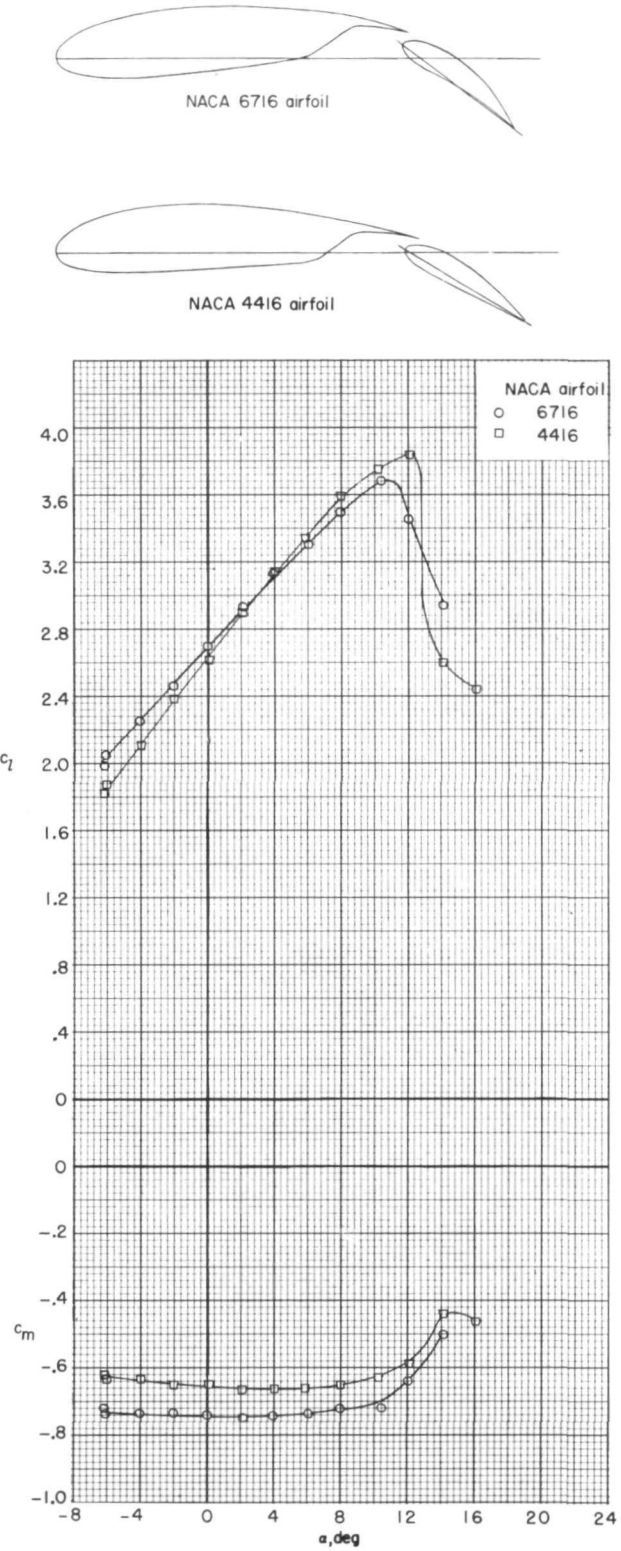


(e) Slot entry 3 sealed; $\delta_f = 0^\circ$.



(f) Slot entry 3; $\delta_f = 30^\circ$.

Figure 8.- Continued.



(g) Slot entry 2; $\delta_f = 30^\circ$.

Figure 8.- Concluded.

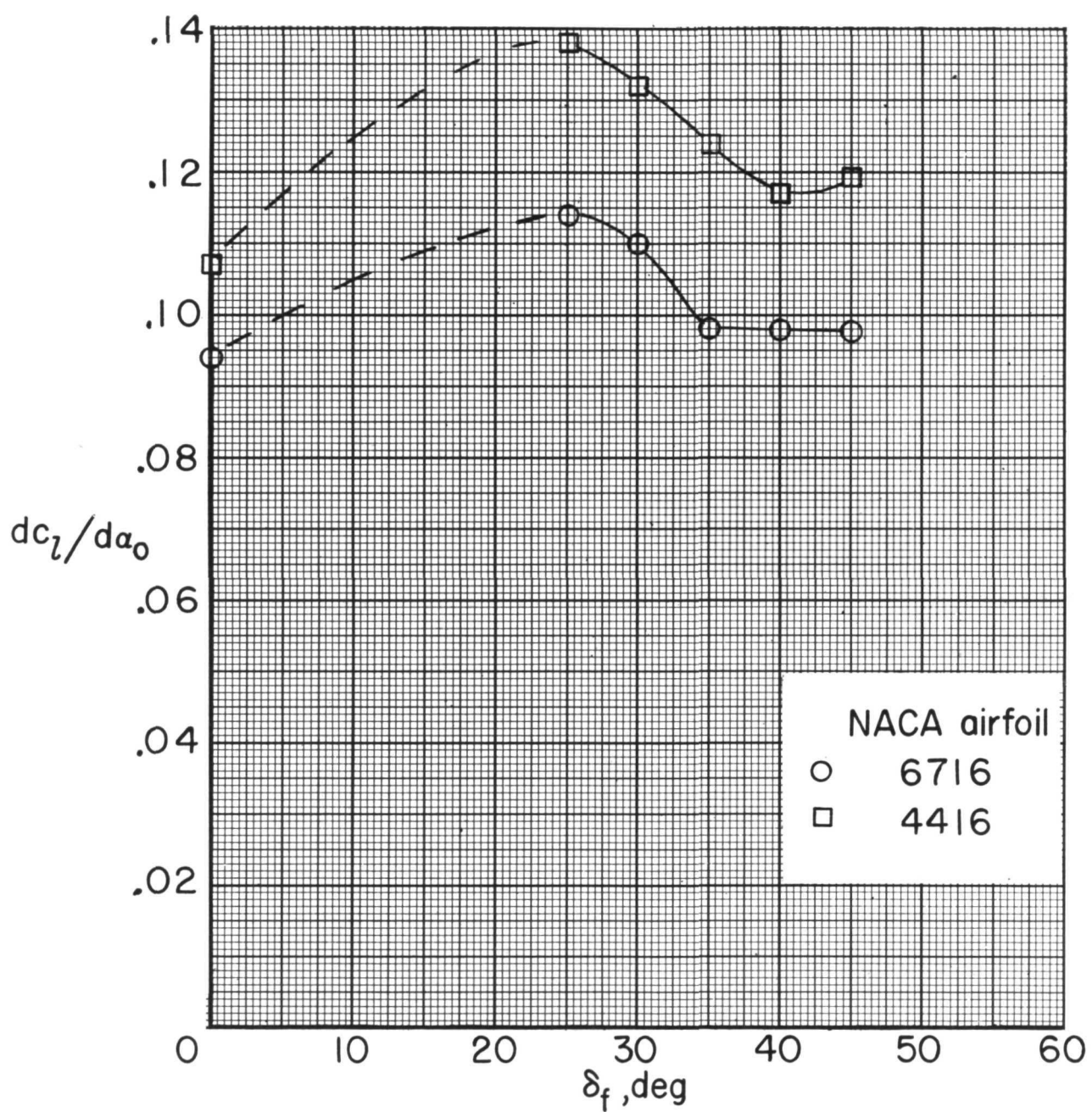
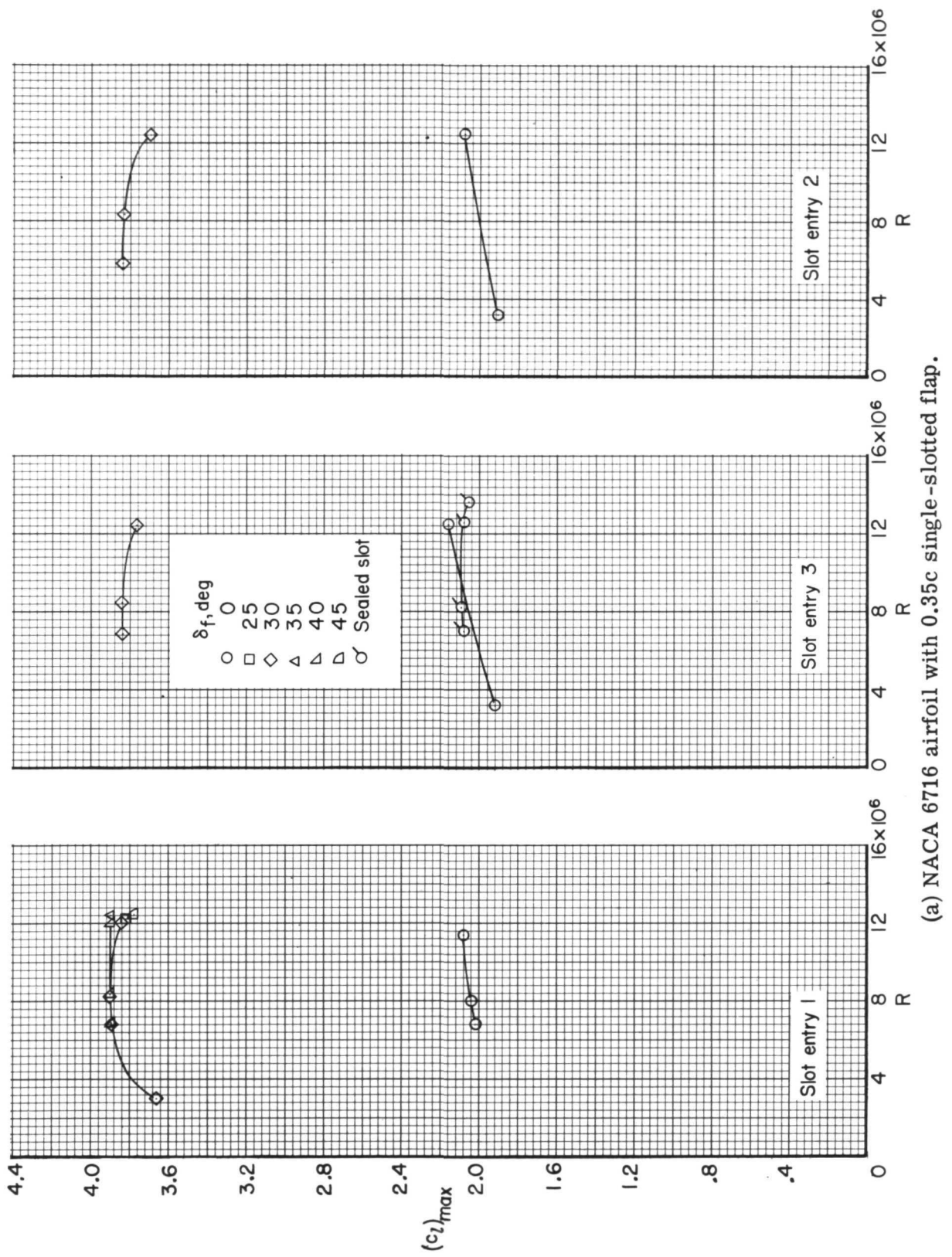
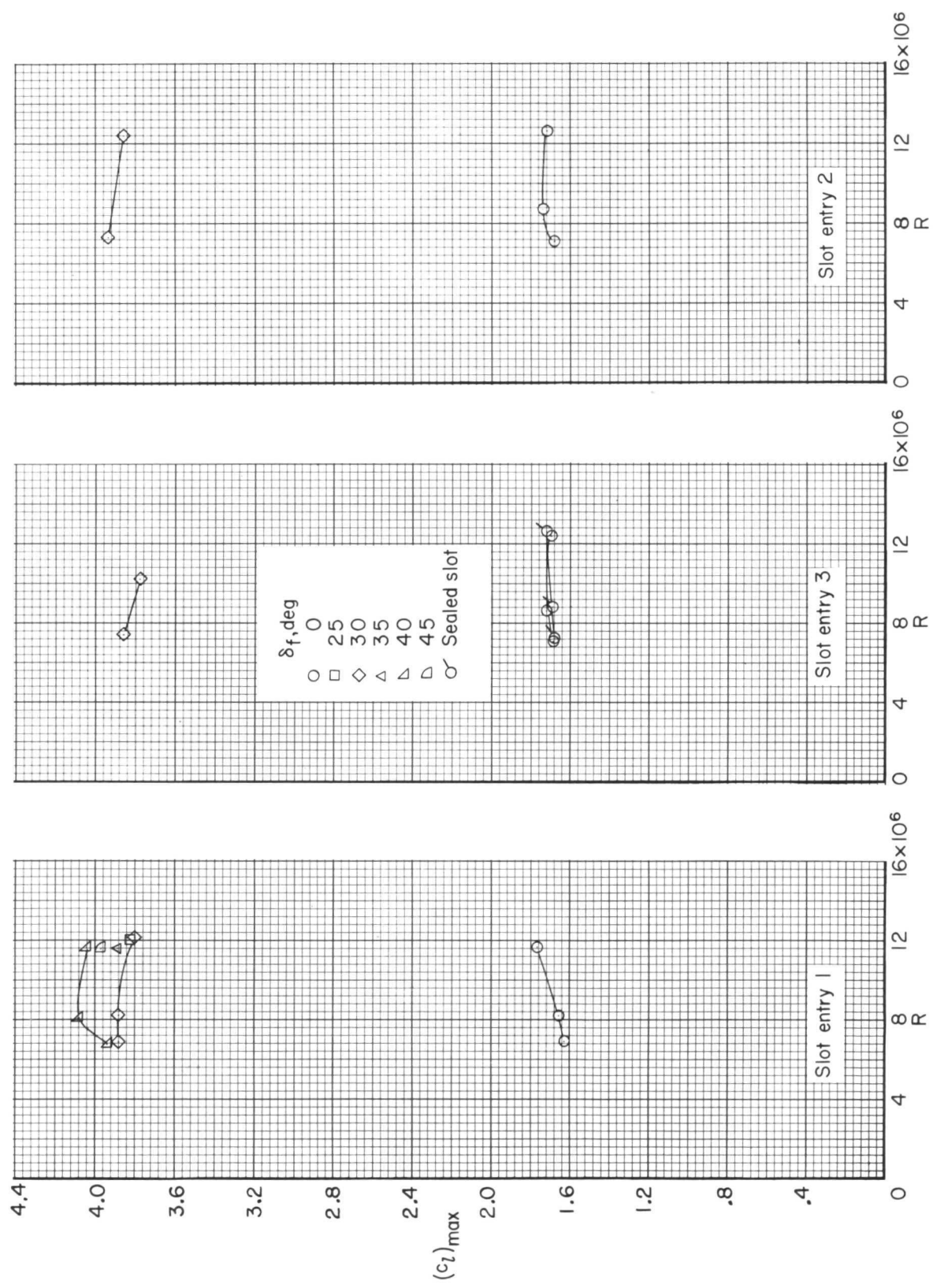


Figure 9.- Variation of lift-curve slope at $\alpha = 0^{\circ}$ with flap deflection angle.
Slot entry 1; $R \approx 12 \times 10^6$; $M = 0.23$.



(a) NACA 6716 airfoil with 0.35c single-slotted flap.

Figure 10.- Variation of maximum section lift coefficient with Reynolds number. $M = 0.23$.



(b) NACA 4416 airfoil with 0.35c single-slotted flap.

Figure 10.- Concluded.

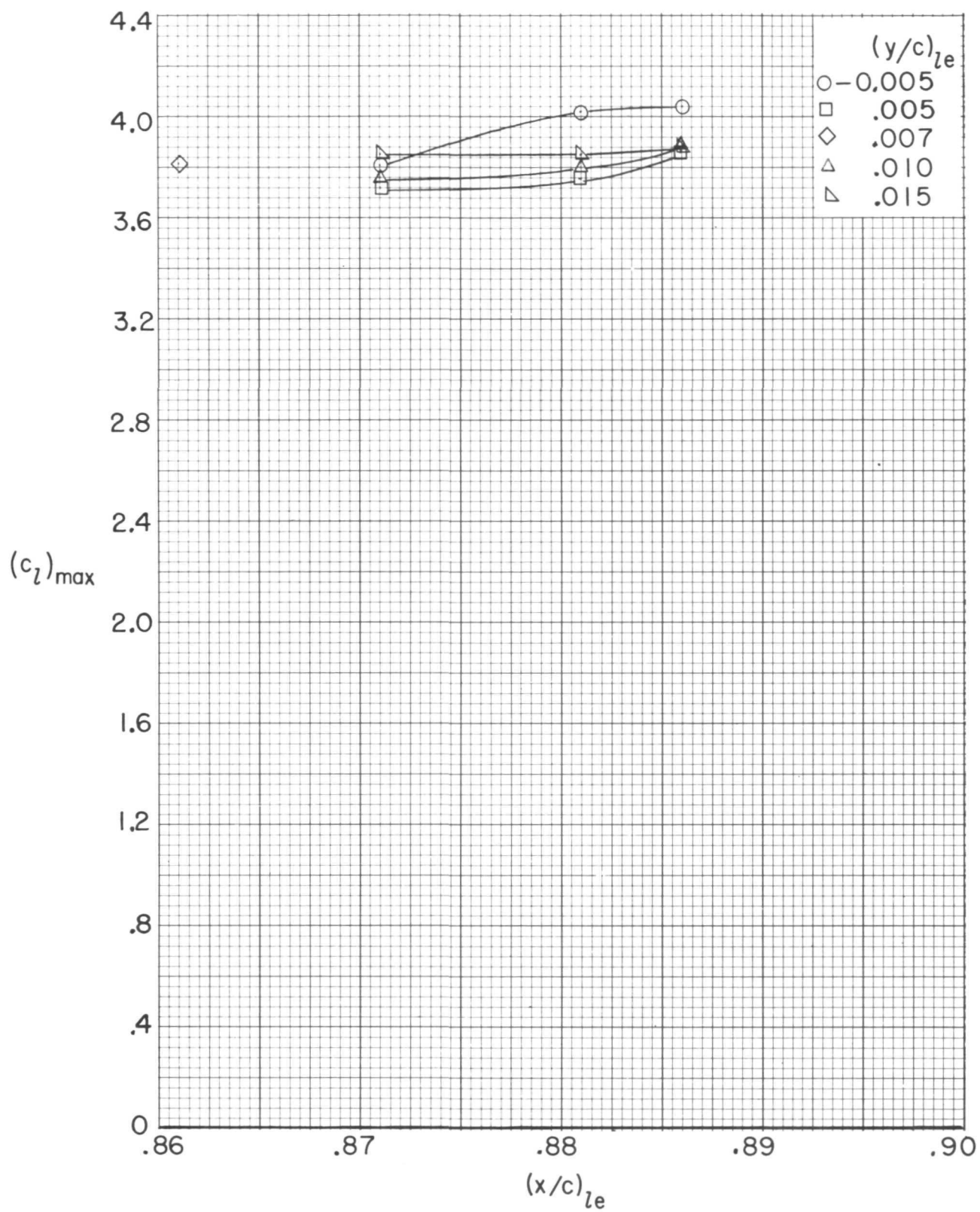


Figure 11.- Effect of flap leading-edge position on maximum section lift coefficient.

NACA 4416 airfoil; slot entry 1; $\delta_f = 30^\circ$; $R \approx 12 \times 10^6$; $M = 0.23$.

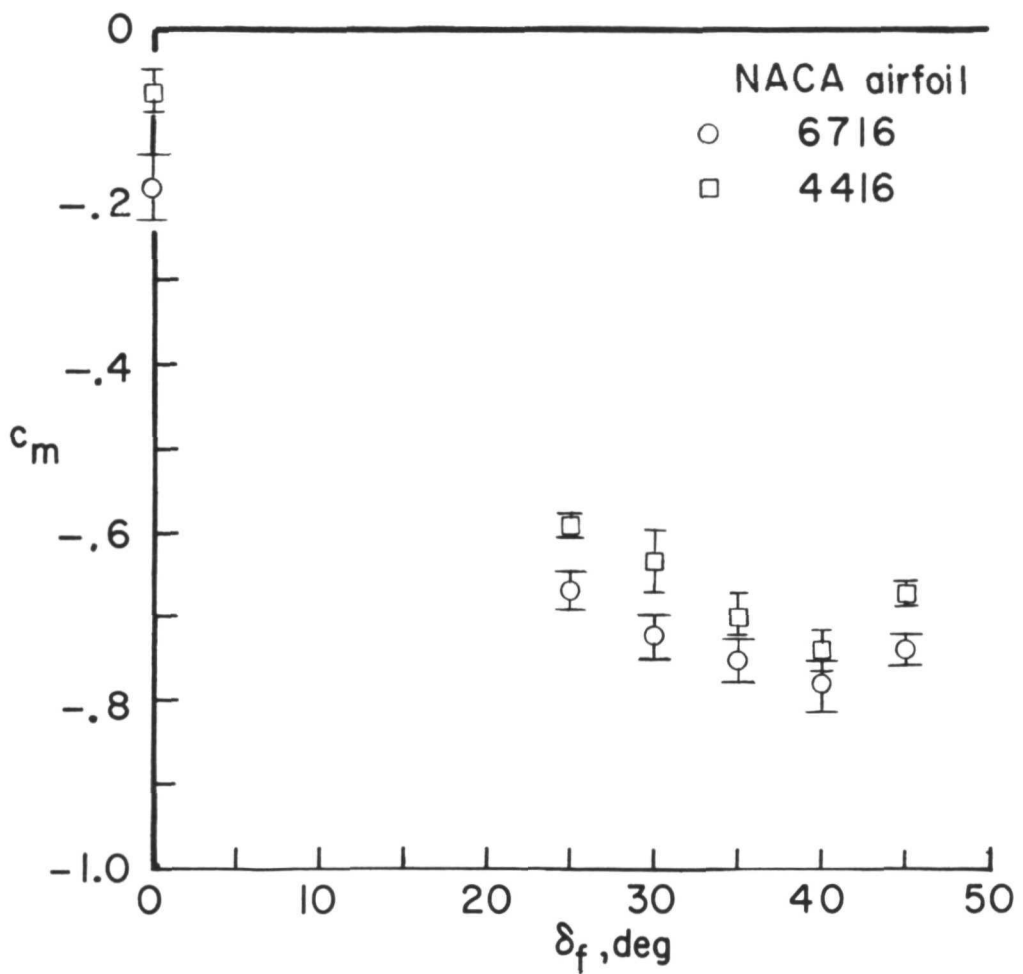
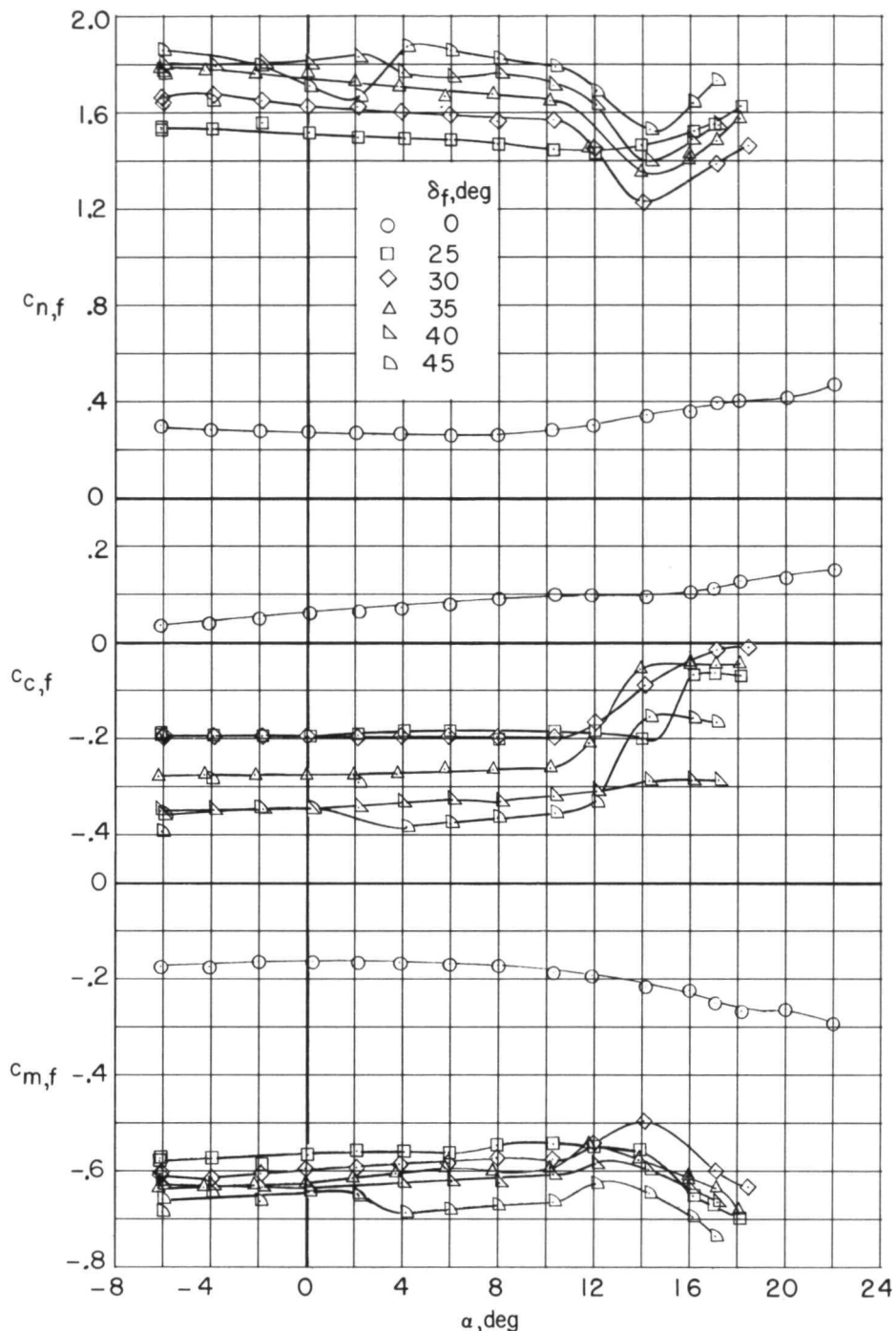
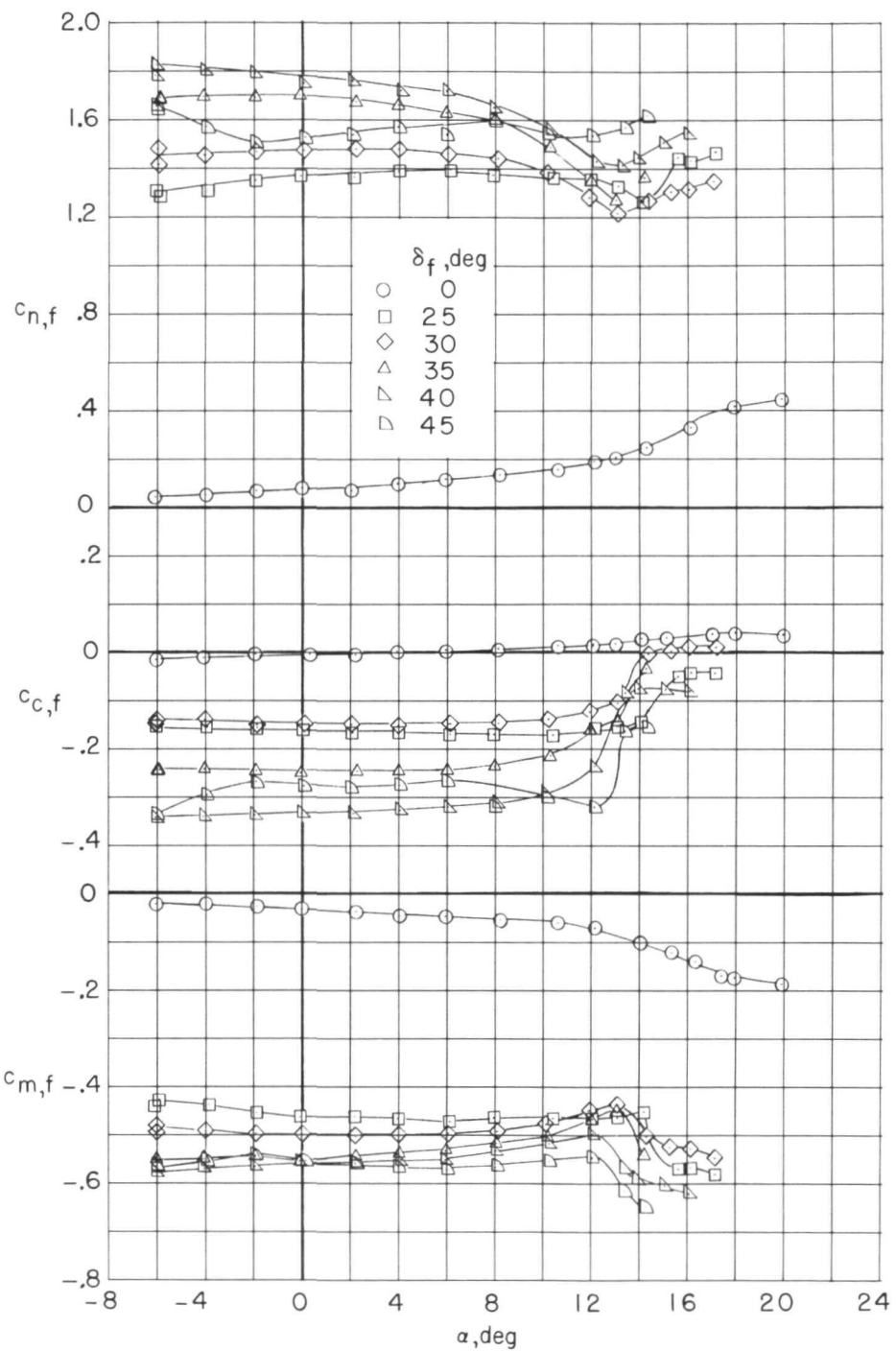


Figure 12.- Variation of section pitching-moment coefficient with flap deflection angle.
 Slot entry 1; $R \approx 12 \times 10^6$; $M = 0.23$. The combined influence of angle of attack
 up to stall, R , and SE shape is indicated by symbol height.



(a) NACA 6716 airfoil.

Figure 13.- Influence of flap deflection angle on section flap pitching-moment, normal-force, and chord-force coefficients. Slot entry 1; $R \approx 12 \times 10^6$; $M = 0.23$.



(b) NACA 4416 airfoil.

Figure 13.- Concluded.

NATIONAL AERONAUTICS AND SPACE ADMINISTRATION
WASHINGTON, D.C. 20546

OFFICIAL BUSINESS
PENALTY FOR PRIVATE USE \$300

SPECIAL FOURTH-CLASS RATE
BOOK

POSTAGE AND FEES PAID
NATIONAL AERONAUTICS AND
SPACE ADMINISTRATION
451



POSTMASTER : If Undeliverable (Section 158
Postal Manual) Do Not Return

"The aeronautical and space activities of the United States shall be conducted so as to contribute . . . to the expansion of human knowledge of phenomena in the atmosphere and space. The Administration shall provide for the widest practicable and appropriate dissemination of information concerning its activities and the results thereof."

—NATIONAL AERONAUTICS AND SPACE ACT OF 1958

NASA SCIENTIFIC AND TECHNICAL PUBLICATIONS

TECHNICAL REPORTS: Scientific and technical information considered important, complete, and a lasting contribution to existing knowledge.

TECHNICAL NOTES: Information less broad in scope but nevertheless of importance as a contribution to existing knowledge.

TECHNICAL MEMORANDUMS: Information receiving limited distribution because of preliminary data, security classification, or other reasons. Also includes conference proceedings with either limited or unlimited distribution.

CONTRACTOR REPORTS: Scientific and technical information generated under a NASA contract or grant and considered an important contribution to existing knowledge.

TECHNICAL TRANSLATIONS: Information published in a foreign language considered to merit NASA distribution in English.

SPECIAL PUBLICATIONS: Information derived from or of value to NASA activities. Publications include final reports of major projects, monographs, data compilations, handbooks, sourcebooks, and special bibliographies.

TECHNOLOGY UTILIZATION PUBLICATIONS: Information on technology used by NASA that may be of particular interest in commercial and other non-aerospace applications. Publications include Tech Briefs, Technology Utilization Reports and Technology Surveys.

Details on the availability of these publications may be obtained from:

SCIENTIFIC AND TECHNICAL INFORMATION OFFICE

NATIONAL AERONAUTICS AND SPACE ADMINISTRATION

Washington, D.C. 20546